

Metadata of the chapter that will be visualized online

Chapter Title	<i>Oikopleura dioica</i> : An Emergent Chordate Model to Study the Impact of Gene Loss on the Evolution of the Mechanisms of Development
Copyright Year	2019
Copyright Holder	Springer Nature Switzerland AG
Author	Family Name Ferrández-Roldán Particle Given Name Alfonso Suffix Division Facultat de Biologia, Departament de Genètica, Microbiologia i Estadística and Institut de Recerca de la Biodiversitat (IRBio) Organization Universitat de Barcelona Address Barcelona, Catalonia, Spain
Author	Family Name Martí-Solans Particle Given Name Josep Suffix Division Facultat de Biologia, Departament de Genètica, Microbiologia i Estadística and Institut de Recerca de la Biodiversitat (IRBio) Organization Universitat de Barcelona Address Barcelona, Catalonia, Spain
Author	Family Name Cañestro Particle Given Name Cristian Suffix Division Facultat de Biologia, Departament de Genètica, Microbiologia i Estadística and Institut de Recerca de la Biodiversitat (IRBio) Organization Universitat de Barcelona Address Barcelona, Catalonia, Spain
Corresponding Author	Family Name Albalat Particle Given Name Ricard Suffix Division Facultat de Biologia, Departament de Genètica, Microbiologia i Estadística and Institut de Recerca de la Biodiversitat (IRBio)

Organization Universitat de Barcelona
Address Barcelona, Catalonia, Spain
Email ralbalat@ub.edu

Abstract

The urochordate *Oikopleura dioica* is emerging as a nonclassical animal model in the field of evolutionary developmental biology (a.k.a. evo-devo) especially attractive for investigating the impact of gene loss on the evolution of mechanisms of development. This is because this organism fulfills the requirements of an animal model (i.e., has a simple and accessible morphology, a short generation time and life span, and affordable culture in the laboratory and amenable experimental manipulation), but also because *O. dioica* occupies a key phylogenetic position to understand the diversification and origin of our own phylum, the chordates. During its evolution, *O. dioica* genome has suffered a drastic process of compaction, becoming the smallest known chordate genome, a process that has been accompanied by exacerbating amount of gene losses. Interestingly, however, despite the extensive gene losses, including entire regulatory pathways essential for the embryonic development of other chordates, *O. dioica* retains the typical chordate body plan. This unexpected situation led to the formulation of the so-called inverse paradox of evo-devo, that is, when a genetic diversity is able to maintain a phenotypic unity. This chapter reviews the biological features of *O. dioica* as a model animal, along with the current data on the evolution of its genes and genome. We pay special attention to the numerous examples of gene losses that have taken place during the evolution of this unique animal model, which is helping us to understand to which the limits of evo-devo can be pushed off.

Chapter 4

Oikopleura dioica: An Emergent Chordate Model to Study the Impact of Gene Loss on the Evolution of the Mechanisms of Development

Alfonso Ferrández-Roldán, Josep Martí-Solans, Cristian Cañestro, and Ricard Albalat

Abstract The urochordate *Oikopleura dioica* is emerging as a nonclassical animal model in the field of evolutionary developmental biology (a.k.a. evo-devo) especially attractive for investigating the impact of gene loss on the evolution of mechanisms of development. This is because this organism fulfills the requirements of an animal model (i.e., has a simple and accessible morphology, a short generation time and life span, and affordable culture in the laboratory and amenable experimental manipulation), but also because *O. dioica* occupies a key phylogenetic position to understand the diversification and origin of our own phylum, the chordates. During its evolution, *O. dioica* genome has suffered a drastic process of compaction, becoming the smallest known chordate genome, a process that has been accompanied by exacerbating amount of gene losses. Interestingly, however, despite the extensive gene losses, including entire regulatory pathways essential for the embryonic development of other chordates, *O. dioica* retains the typical chordate body plan. This unexpected situation led to the formulation of the so-called inverse paradox of evo-devo, that is, when a genetic diversity is able to maintain a phenotypic unity. This chapter reviews the biological features of *O. dioica* as a model animal, along with the current data on the evolution of its genes and genome. We pay special attention to the numerous examples of gene losses that have taken place during the evolution of this unique animal model, which is helping us to understand to which the limits of evo-devo can be pushed off.

Alfonso Ferrández-Roldán and Josep Martí-Solans contributed equally with all other contributors.

A. Ferrández-Roldán · J. Martí-Solans · C. Cañestro · R. Albalat (✉)
Facultat de Biologia, Departament de Genètica, Microbiologia i Estadística and Institut de Recerca de la Biodiversitat (IRBio), Universitat de Barcelona, Barcelona, Catalonia, Spain
e-mail: ralbalat@ub.edu

© Springer Nature Switzerland AG 2019

W. Tworzydło, S. M. Bilinski (eds.), *Evo-Devo: Non-model Species in Cell and Developmental Biology*, Results and Problems in Cell Differentiation 68,
https://doi.org/10.1007/978-3-030-23459-1_4

AU1

4.1 Introduction

34 In 1872, the Swiss marine biologist Hermann Fol during his stay in Messina (Sicilia,
35 Italy) described a new planktonic species of Urochordates (a.k.a. Tunicates), the
36 appendicularian (a.k.a. Larvacean) *Oikopleura dioica* (Fol 1872). From the begin-
37 ning, *O. dioica* exhibited interesting biological features because, using Fol's own
38 words, "Je n'ai jamais trouvé sur un meme individu les organes male et femelle.
39 Notre espece est réellement un tunicier a sexes distincts" (I have never found on the
40 same individual the male and female organs. Our species is really a tunicate with
41 distinct sexes) (Fol 1872). This was a remarkable finding because until then, it was
42 assumed that Urochordates were hermaphrodites. At the beginning of the twentieth
43 century, the Russian embryologist Vladimir Vladimirovich Salensky (commonly
44 known as W. Salensky) described the anatomy of different Appendicularia species
45 (Salensky 1903, 1904, 1905). Although in 1903 Richard Benedict Goldschmidt
46 provided a first brief description of the larva of *O. dioica* (Goldschmidt 1903), the
47 Dutch biologist Hendricus Christoffel Delsman can be considered the father of
48 *O. dioica* embryogenesis. He, analyzing embryos directly collected from the field,
49 was able to laboriously reconstruct its cleavage pattern with amazing exactitude
50 (Delsman 1910, 1912), which a century later has been confirmed by confocal
51 microscopy and live imaging (Fujii et al. 2008; Stach et al. 2008).

52 During the 1960s and 1970s, the *O. dioica* anatomy was described in deep detail,
53 paying special attention to some conspicuous structures such as the notochord or the
54 endostyle (Olsson 1963, 1965a, b; Welsch and Storch 1969) and to the organs
55 required for the construction and use of the "house," a filtering complex structure
56 that traps the food (Galt 1972). Almost at the same time, the first *O. dioica* cultures in
57 the laboratory were successfully maintained through numerous generations
58 (Paffenhöfer 1973), and over the next 30 years, numerous ecological and biogeo-
59 graphical studies were reported (e.g., Galt 1978; King et al. 1980; Gorsky et al. 1984;
60 Bedo et al. 1993; Acuña et al. 1995; Hopcroft and Roff 1995; Uye and Ichino 1995;
61 Nakamura et al. 1997; Hopcroft et al. 1998) along with multiple morphological,
62 anatomical, and physiological descriptions (e.g., Last 1972; Bone and Mackie 1975;
63 Olsson 1975; Fenaux 1976, 1986; Flood and Afzelius 1978; Fredriksson and Olsson
64 1981, 1991; Holmberg 1982, 1984; Fredriksson et al. 1985; Bollner et al. 1986;
65 Georges et al. 1988; Holland et al. 1988; Olsson et al. 1990; Nishino and Morisawa
66 1998; Lopez-Urrutia and Acuña 1999; Acuña and Kiefer 2000).

67 All this accumulated knowledge led *O. dioica* to the twenty-first century, when
68 shotgun sequencing techniques (Seo et al. 2001; Denoëud et al. 2010) together with
69 the establishment of protocols for gene expression analysis (Bassham and
70 Postlethwait 2000; Nishino et al. 2000) paved the groundwork for *O. dioica* as a
71 promising nonclassical model species for different biological disciplines, including
72 comparative genomics, molecular genetics, or evolutionary developmental biology
73 (evo-devo). Here, we will review the main biological features of *O. dioica* as
74 chordate model at the morphological, physiological, embryonic, ecological, meth-
75 odological, evolutionary, genetic, and genomic levels, paying special attention to the

fact that *O. dioica* has shrunk and compacted its genome retaining the archetypical chordate body plan. We will finish by analyzing the impact of gene loss, especially the loss of genes related to embryonic development, on the evolution of *O. dioica*.

4.2 *Oikopleura dioica* as a Nonclassical Model System for Evo-Devo

A model organism is a simplified and accessible system that represents a more complex entity, based on the notion summarized by Jacques Monod: “what is true for *E. coli* is true for the elephant.” This notion reflects the evolutionary principle that all organisms share some degree of functional and genetic similarity due to common ancestry. There are several classical model species in cell and developmental biology, from non-vertebrates such as the roundworm *Caenorhabditis elegans* or the fruit fly *Drosophila melanogaster* to vertebrates such as zebrafish and mouse. The choice of a particular model organism depends, essentially, on the specific scientific question that needs to be investigated, and new scientific questions usually demand new model systems. Thus, when we became interested to understand the impact of the gene loss on the evo-devo of chordates, we had to look for a new “nonclassical” model system suitable for our studies. *O. dioica* was our first choice because it has many technical and biological advantages that made it attractive for our objectives: (1) *O. dioica* has a simple and accessible morphology, maintaining the typical chordate body plan throughout its life; (2) its generation time and life span is short with a fast, invariant, and determinative embryonic development; (3) *O. dioica* is easily accessible and affordably cultured; (4) *O. dioica* can be experimentally manipulated; (5) *O. dioica* occupies a privileged phylogenetic position within the chordates to better understand the evolution of our own phylum; and (6) its genome is small, compacted, and prone to lose genes. In the next sections, we will summarize these technical and biological advantages.

4.2.1 *O. dioica* Is a Morphologically Simple Animal with Typical Chordate Body Plan

O. dioica has a simple but typical chordate body plan with organs and structures that are unequivocally homologous to those in vertebrates and other chordates, including a notochord anchoring muscle cells along a postanal tail, a hollow neural tube that becomes a central nervous system (CNS) organized in two big ganglia and a nerve cord, as well as a pair of gill slits and an endostyle in the pharyngeal region, which connects with the digestive tract (Fig. 4.1). The body of *O. dioica* is divided in two parts, the trunk (0.12–0.85 mm), which contains most of the organs, and the tail (1.2–3.2 mm), which contains the notochord, the tail nerve cord, and two rows of

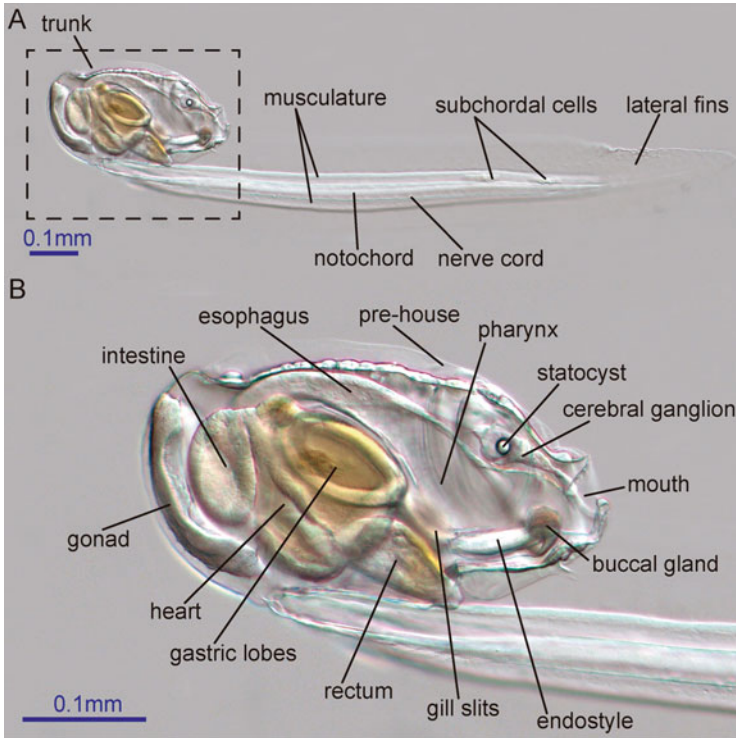


Fig. 4.1 Immature adult specimen of *O. dioica*. (a) Differential interference contrast (DIC) micrograph in right lateral view with anterior to the left and ventral down. (b) Magnification of the trunk showing the main organs and structures. Bar: 0.1 mm

112 paired muscle cells. The whole body is transparent so the inner structures can be
 113 visualized by simply changing the focal plane of the microscope.

114 4.2.1.1 Nervous System

AU3

115 The CNS of *O. dioica* is made by only approximately 100 cells. Despite this
 116 extremely simple structure, *O. dioica* CNS shows homology with the vertebrate
 117 forebrain, hindbrain, and spinal cord of vertebrates (but not the midbrain) (Cañestro
 118 et al. 2005). The CNS of *O. dioica* comprises a nerve cord running along the tail and
 119 two big ganglia (i.e., the cerebral ganglion in the most anterior part of the trunk and
 120 the caudal ganglion in the most proximal region of the tail) (Holmberg 1984). Both
 121 ganglia secrete gamma-aminobutyric acid (GABA) (Soviknes et al. 2005). The
 122 cerebral ganglion, proposed to be homologous to the vertebrate forebrain (Cañestro
 123 et al. 2005), is made of approximately 70 neurons and includes a statocyst, a balance
 124 sensory receptor in which a mineralized mass called statolith pushes a group of
 125 ciliary cells in response to gravity, providing therefore feedback to the animal on

change in orientation (Holmberg 1984) (Fig. 4.1). The cerebral ganglion connects with sensory cells in the mouth, the pharynx, and the ventral organ (a simple structure of about 30 cells homologous to the olfactory placode and the pituitary of vertebrates) (Bollner et al. 1986; Cañestro et al. 2005) and integrates the information received from the sensory cells. The cerebral ganglion also connects to the caudal ganglion through the trunk nerve cord, which turns to the right before entering the tail. Caudal ganglion and trunk nerve cord have been proposed to be homologous to at least part of vertebrate hindbrain (Cañestro et al. 2005). The caudal ganglion and the nerve cord that runs along the tail consist of approximately 30 neurons. Along the nerve cord, neuronal nuclei are collected in groups of two to four forming small ganglia. Small fibers arising from these ganglia innervate the symmetric musculature of the tail with cholinergic motoneurons and coordinate its movements (Galt 1972; Soviknes and Glover 2007).

4.2.1.2 Epidermis and Secreted “House”

The epidermis is a monolayered epithelium without any underlying mesodermal tissue that covers the whole body of *O. dioica* (Nishida 2008). The epidermis of the trunk, called oikoblast or oikoplastic epithelium, contains a fixed number of cells (approximately 2000) organized in different domains defined by the shape of the cells and the morphology of their nuclei and showing a complex bilateral symmetric pattern (Thompson et al. 2001; Kishi et al. 2017; Mikhaleva et al. 2018) (Fig. 4.2a). The oikoplastic epithelium secretes the so-called house, a filter-feeding device made of glycopolysaccharides, mucopolysaccharides, and cellulose (Fig. 4.2b, c) (Kimura et al. 2001; Spada et al. 2001; Thompson et al. 2001). The distribution of the epidermal cells of the trunk has a direct correlation with the different architectonic structures of the house (Fig. 4.2a) (Spada et al. 2001; Thompson et al. 2001; Kishi et al. 2017). The adult specimens of *O. dioica* live inside this mucous house (Fig. 4.2b, c) that works as a food-trapping device by filtering picoplankton particles of different sizes (from 0.1 to 50 μm) from the water stream propelled by stylish and grooving tail movements (Fenaux 1986; Thompson et al. 2001). The house is abandoned when the filters are obstructed, and a new one is immediately inflated, which happens between four and ten times a day increasing with higher water temperatures (Flood and Deibel 1998; Sato et al. 2003). This energetically exhausting strategy has been proposed as an evolutionary adaptation to poor food environments (Acuña et al. 2002).

4.2.1.3 Pharyngeal Region and Digestive Tract

The food particles caught by the house enter through the mouth situated at the anterior region of the trunk to the pharynx, thanks to the water flux generated by the spiracles, a pair of gill slits with beating cilia that generate a water stream into the body to draw the food (Fenaux 1998a) (Fig. 4.3). Within the pharynx, food particles

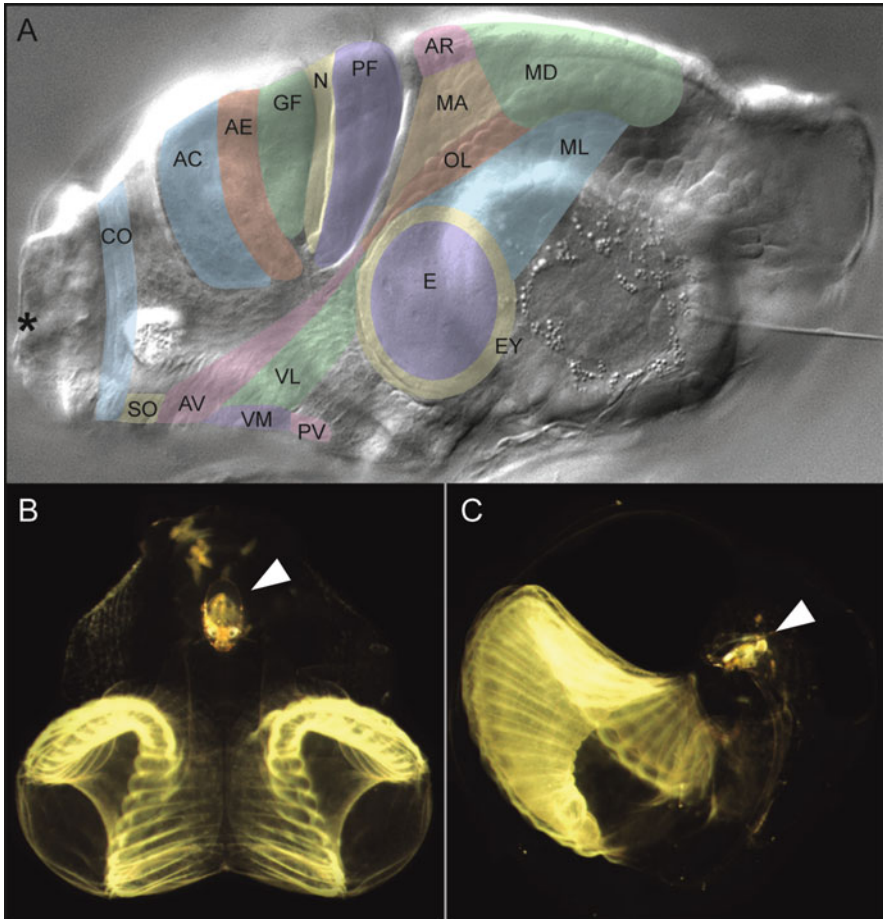


Fig. 4.2 The *O. dioica* epidermis and the secreted house. Lateral view of an *O. dioica* trunk, in which the main domains of the oikoplastic epithelium that correlate with the different architectonic structures of the house are depicted (a): AC anterior crescent, AE anterior elongated region, AR anterior rosette, AV anterior ventral domain, CO circumoral domain, E Eisen giant cells, EY Eisen's yard, GF giant Fol, MA martini, ML mid-lateral domain, MD middorsal domain, N nasse, OL oblique line, PF posterior fol, PV posterior ventral domain, SO sensory organ, VL ventrolateral domain, VM ventromedial domain. AC, AE, GF, N, and PF form the fol domain (Kishi et al. 2017). Anterior is to the left and ventral down. The asterisk indicates the mouth. Frontal (b) and lateral (c) views of the *O. dioica* house, which is visible thanks to the algae trapped in the structure. The trunk of the animal inside the house is also visible (arrowhead)

165 are trapped by the mucus that covers its walls. The mucus is secreted by the
 166 endostyle, an organ homologous to the thyroid of vertebrates, and localized on the
 167 ventral side of the pharynx (Olsson 1963; Cañestro et al. 2008). This mucus is
 168 conducted to the digestive tract by two symmetric rows of cilia at the lateral walls of
 169 the pharynx that finally meet at the superior region (Fenaux 1998a). The digestive

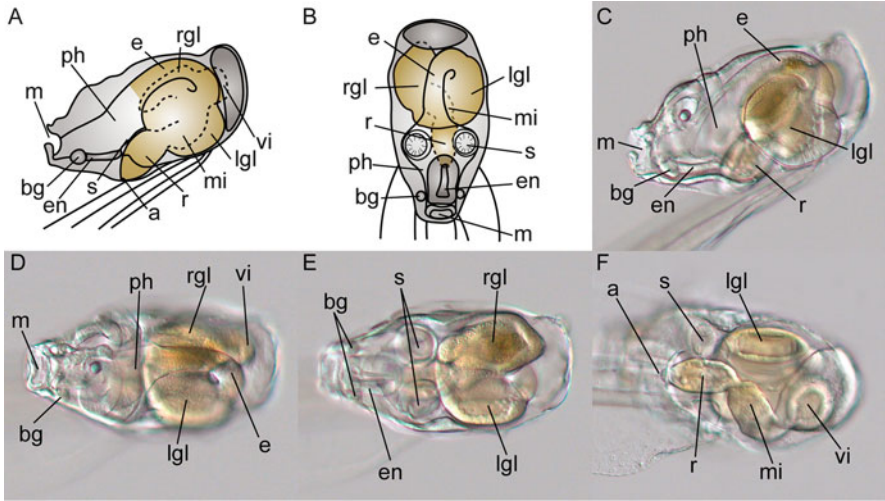


Fig. 4.3 Pharyngeal region and digestive system in the *O. dioica* trunk. Diagrams of the trunk and anatomy of the pharyngeal region and digestive tract of *O. dioica* from the left (a) and dorsal (b) views. DIC micrographs of the trunk of an *O. dioica* adult specimen in left lateral view (c), dorsal views at two different focal planes (d, e), and ventral view (f). Anterior is to the left. Anus (a), buccal gland (bg), endostyle (en), esophagus (e), left gastric lobe (lgl), mid-intestine (mi), mouth (m), pharynx (ph), rectum (r), right gastric lobe (rgl), spiracles (s), and vertical intestine (vi)

tract is composed of an esophagus, two gastric lobes (right and left stomachs), and a bent intestine divided in vertical, mid, and distal intestine (or rectum) (Burighel and Brena 2001; Cima et al. 2002) (Fig. 4.3). Although the absorption of liquids, ions, and small molecules takes place all over the digestive system (Burighel and Brena 2001), different compartments have different functions. Digestive enzymatic activity, for instance, is led mainly by the left gastric lobule where different enzymes such as α -amylase, acid phosphatase, nonspecific esterase, 5'-nucleotidase, and aminopeptidase M are released (Cima et al. 2002). In contrast, accumulation of lipid droplets in ciliated cells of the right gastric lobule and the vertical and mid-intestine indicates a storage role for these compartments (Cima et al. 2002). Finally, fecal pellets are formed in the vertical intestine and transit along the intestine allowing protein absorption by the rectal granular cells (Burighel and Brena 2001; Cima et al. 2002), until reaching the anus where they are released. Functional compartmentalization is further supported by spatiotemporal differences in the onset of gene expression during the development of the digestive system (Martí-Solans et al. 2016), likely reflecting processes of functional differentiation and specialization of digestive cells.

170
171
172
173
174
175
176
177
178
179
180
181
182
183
184
185
186

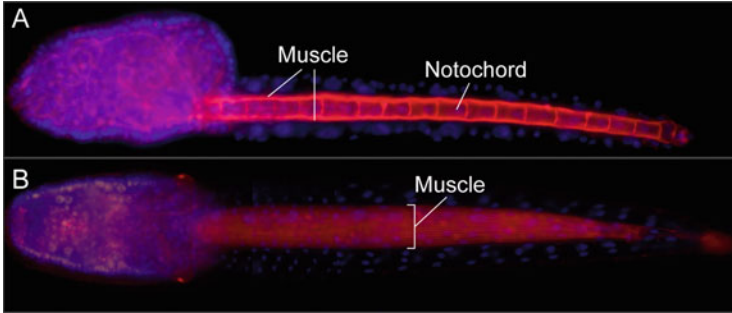


Fig. 4.4 Notochord and tail musculature in an *O. dioica* larva. These two tissues stand out over the general phalloidin staining of the actin filaments (in red), and they spread from the base of the trunk to the posterior tip. In lateral view, notochord is in the center of the tail flanked by two strips of striated muscle cells located on dorsal and ventral sides (a). In ventral view, sarcomeres are distinguished as repeated structures all along the strip of muscle cells (b). Nuclei are stained with Hoechst (in blue). Anterior is to the left

187 4.2.1.4 Notochord and Subchordal Cells

188 The notochord is a synapomorphic structure of the chordate phylum (Sato et al.
 189 2012) that has a dual function: providing structural support to the developing
 190 embryo and secreting patterning signals required for tissue specification and organ-
 191 ogenesis (Cleaver and Krieg 2001). In *O. dioica*, the notochord is a row of cells or
 192 “stack of coins” that runs along the tail (Figs. 4.1 and 4.4). During larval develop-
 193 ment, notochord cells form vacuoles that eventually coalesce to form a hollow lumen
 194 (Soviknes and Glover 2008). In the adult, the notochord is a tube of cells with thin
 195 walls, whose cells secrete proteins rich in sulfur to the extracellular media to keep the
 196 stiffness of the notochord, but also flexible enough to facilitate swimming and other
 197 movements (Olsson 1965a). The genetic toolkit to build the notochord in *O. dioica*
 198 has been investigated, revealing not only similarities but also significant differences
 199 in the complement of genes employed by different chordates (Ferrier 2011; Kugler
 200 et al. 2011). The evolutionary origin of the notochord is a hot topic of discussion, and
 201 the analysis of the *O. dioica* notochord has contributed to corroborate that the
 202 urochordate noncontractile actin-expressing notochord may represent the ancestral
 203 condition in stem chordates (Almazán et al. 2018; Inoue and Sato 2018).

204 At the right side of the notochord, there is a pair of conspicuous cells, the
 205 so-called subchordal cells (Fol 1872; Delsman 1910; Lohmann 1933) (Fig. 4.1).
 206 These cells migrate during *O. dioica* development from the trunk to the tip of the tail,
 207 at the same time that the endodermal strand cells enter the trunk following the same
 208 path but in opposite directions (Kishi et al. 2014). Subchordal cells together with
 209 endodermal strand cells and oral gland cells are three cell populations exhibiting
 210 long-distance migration during *O. dioica* development (Kishi et al. 2014), two of
 211 them—the subchordal and the endodermal strand cells—likely sharing the same
 212 origin (Fredriksson and Olsson 1991). The function of the subchordal cells remains
 213 elusive, although it has been proposed that they may be involved in the exchange of

materials with the body fluid, from which they pick and transform substances in a hepatic-like process (Fredriksson and Olsson 1991). These substances can either be changed into low molecular weight products merely for detoxification of harmful substances or be metabolized into new, useful molecules that are released back to the hemolymph (Fredriksson and Olsson 1991; Fenaux 1998a).

4.2.1.5 Heart and Tail Musculature

In *O. dioica*, muscle cells are only found in the heart and in the tail. They are in both cases striated muscle cells showing the characteristic repeating functional units called sarcomeres (Onuma et al. 2017; Almazán et al. 2018) (Fig. 4.4b), while the existence of smooth muscle cells in *O. dioica* has not been established so far. *O. dioica* heart is the simplest chordate heart, and assisted by the tail movement, it contributes to the circulation of the hemolymph between the ectoderm and the internal organs in an open circulatory system (Fenaux 1998a). The heart consists of a posterior ventral bag wedged between the left stomach wall and the intestine (Fig. 4.1). The internal lumen of this bag is the only coelomic space in *O. dioica*, and it is completely lined by two types of flat mesodermal tissues, the myocardium composed by muscle fibers and the nonmuscular pericardium (Stach 2009; Onuma et al. 2017). Myocardial cells are connected by cell junctions, and their cytoplasm is full of actin filaments (Stach 2009; Onuma et al. 2017; Almazán et al. 2018). This muscle-structured tissue produces peristaltic contractions that periodically reverse, causing the hemolymph to course between the myocardium and the stomach wall reaching the rest of the organs in the trunk and circulating through the tail (Fenaux 1998a).

The muscular tissue of the tail spreads posteriorly from the base of the trunk in two strips of striated cells distributed in the dorsal and ventral sides of the notochord (Nishino et al. 2000; Nishino and Satoh 2001; Almazán et al. 2018) (Fig. 4.4). This paraxial musculature, combined with the notochord, provides the ability to drive movement to the tail, which is fundamental not only for locomotion but also for *O. dioica* feeding. The tail musculature of *O. dioica* consists of only ten multinucleated striated cells on the dorsal and ventral sides of the notochord (Nishino et al. 2000; Nishino and Satoh 2001; Soviknes et al. 2007; Almazán et al. 2018). In just hatched larvae, eight mononucleated muscular cells are easily recognizable along the anterior–posterior axes of the tail. Along the larval development, two additional small muscle cells appear at the tip of the tail although their origin remains unknown (Nishino and Satoh 2001).

Structurally, the actomyosin contractile complexes of the muscle cells in *O. dioica* have not been fully characterized, but actin and myosin genes can be identified in the *O. dioica* database (Almazán et al. 2018). *O. dioica* has four muscular-actin genes that appear to be expressed only in the muscle cell lineage (Almazán et al. 2018). The four muscular actins show differences in their expression domains during embryonic development, which suggests differences in their spatio-temporal regulation (Almazán et al. 2018). Muscular actin expression can be

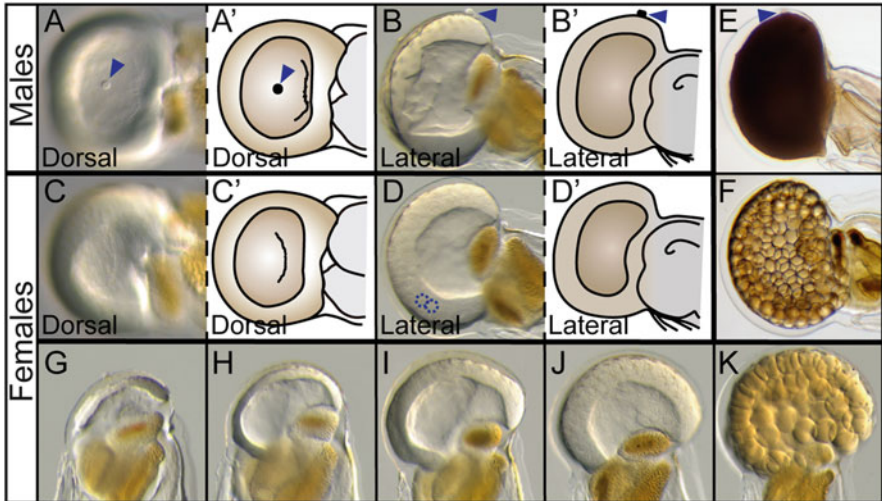


Fig. 4.5 Maturation of male and female gonads. DIC micrographs and schematic representations of dorsal (**a–a'**) and lateral (**b–b'**) views of a premature male gonad. The sperm duct appears as a small protuberance in the most dorsal part of the male gonad (arrowhead). DIC micrographs and schematic representations of dorsal (**c–c'**) and lateral (**d–d'**) views of a premature female ovary. Pro-oocytes can be distinguished inside the gonad (dashed circles). DIC micrographs of mature male (**e**) and female (**f**) gonads. Mature male gonads become brown and opaque as spermatogenesis progresses, while female gonads become yellowish and refringent until the round eggs are clearly visible (**g–k**)

256 detected as early as at 64-cell stage, although muscle fibers are formed later in the
 257 larvae. They are restricted to the inner part of the cell, while the epidermal side is full
 258 of mitochondria generating the energy for the tail movement (Nishino et al. 2000;
 259 Almazán et al. 2018). Comparative analyses among different chordate species,
 260 including *O. dioica*, have suggested that muscular actins originated from a cytoplas-
 261 mic actin at the base of chordates, which was followed by the recruitment of the
 262 myosin motor-machinery that conferred contractile capability to muscle cells
 263 (Kusakabe et al. 1997; Almazán et al. 2018; Inoue and Satoh 2018).

264 4.2.1.6 Reproductive System

265 *O. dioica* is the sole dioecious species so far reported in the urochordate subphylum
 266 (Fol 1872; Nishida 2008). The gonad is localized in the posterior region of the trunk
 267 and is the only apparent character that allows us to differentiate males from females:
 268 male gonad is full of sperm and homogenously brown and dark, whereas the female
 269 one is yellowish and refringent as it is full of eggs (Fig. 4.5). The growth of the
 270 gonad is parallel to the growth of the animal, acquiring their final size and maturity in
 271 only some hours, when gametogenesis occurs (Nishino and Morisawa 1998; Ganot
 272 et al. 2007). Spermatogenesis takes place in the testicle, a syncytium with a

substantial number of identical nuclei that become individual spermatozoa 273
(Martinucci et al. 2005; Onuma et al. 2017). The ovary has also an initial phase of 274
syncytial nuclear proliferation. Then, it becomes a coenocyst where half of the nuclei 275
enter meiosis, whereas the other half became highly polyploid nurse nuclei (Ganot 276
et al. 2007). Inside the coenocyst, a ramified structure composed of filamentous actin 277
surrounds each of the pro-oocytes that are connected to the common cytoplasm via 278
intercellular bridges termed also ring canals (Ganot et al. 2007). During oogenesis a 279
subset of pro-oocytes grows by transferring the cytoplasm through the ring canals 280
while the others degenerate (Ganot et al. 2007). Typically, a mature female spawns 281
between 100 and 400 eggs, although as a clutch manipulator, *O. dioica* females 282
might increase or decrease the oocyte number depending on favorable or unfavor- 283
able environmental conditions, respectively (Troedsson et al. 2002). This feature can 284
be useful to manipulate the clutch size in laboratory conditions. 285

4.2.2 *O. dioica* Has a Short Generation Time and a Determinative Embryonic Development 286 287

A convenient characteristic shared by many model organisms is that their generation 288
time (i.e., the time between two consecutive generations) is short, facilitating genetic 289
analyses through generations. The generation times of *D. melanogaster* and 290
C. elegans, for instance, are of only 9 and 3 days, respectively. The generation 291
time of *O. dioica* is also short, from 5 days at 19 °C to 10 days at 13 °C (Nishida 292
2008; Bouquet et al. 2009; Martí-Solans et al. 2015). After the external fertilization, 293
the zygote starts embryonic development, which lasts 3.5–6.0 h at 19 °C and 13 °C, 294
respectively, and terminates when a larva hatches breaking the chorion (Fig. 4.6). 295
Next, larval development starts; it takes 6–13 h (at 19 °C–13 °C, respectively) and 296
terminates with a 120° twist of the tail at the tailshift stage. Ten minutes later, the 297
juvenile makes its first house and starts feeding. During the next few days, animals 298
filtrate water and feed arriving to the 1.5–4.0 mm of body size for an adult animal. At 299
that point, the gonads complete their maturation, and males and females spawn the 300
gametes and, as semelparous animals, die afterwards (Fig. 4.6). 301

In vitro fertilization protocols (Fenaux 1976; Holland et al. 1988; Nishino and 302
Morisawa 1998) have enabled the understanding of processes that lead the egg to 303
become a larva. Cleavage patterns, cell lineages, and morphogenetic movements, 304
which are especially important for the understanding of the embryology of organ- 305
isms that follow an invariant and determinative embryonic development such as 306
those of *O. dioica*, have been extensively studied (reviewed in Nishida and Stach 307
2014). Thus, fate maps from one cell to the tail bud stage have been established 308
(Fig. 4.7), similarly to what has been made in other organisms as the nematode 309
C. elegans or the ascidian *Ciona robusta* (formerly *C. intestinalis*) (Sulston et al. 310
1983; Nishida 1987; Fujii et al. 2008; Stach et al. 2008; Nishida and Stach 2014; 311
Stach and Anselmi 2015). After fertilization, the surface of the egg becomes rough, 312

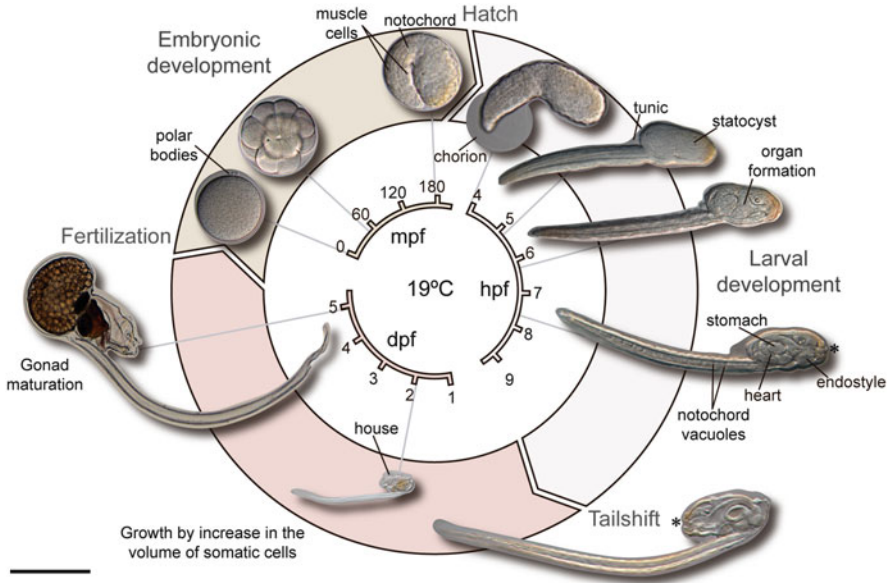


Fig. 4.6 Schematic representation of *O. dioica* life cycle. Embryonic development starts with the fertilization of the oocyte and ends when a larva hatches breaking the chorion (≈ 3.6 hpf at 19°C). Larval development lasts for ≈ 6 h (at 19°C) and ends when the tail of the larva changes 120° its orientation in a process called tailshift. Notice the change of the position of the mouth (asterisk) relative to the tail in juvenile animals. During the next ≈ 4.5 days (at 19°C), juvenile animals feed, grow, and become mature males or females, which spawn the gametes closing the cycle. Scale bar represents $100\ \mu\text{m}$ for all stages except for day 2 and mature adults ($1\ \text{mm}$)

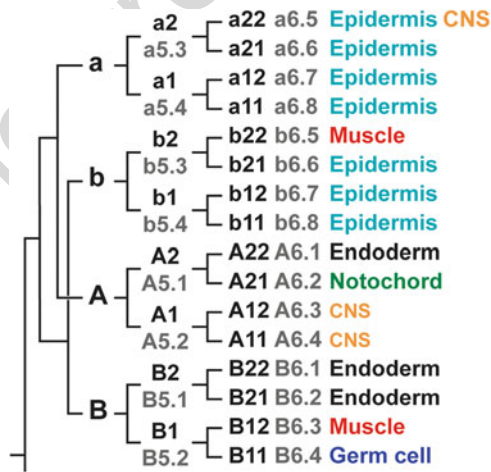


Fig. 4.7 Cell-lineage tree of *O. dioica* embryos. The tree is bilaterally symmetric, and therefore, only one-half is shown. The nomenclature agrees with that of Delsman (1910) and reviewed in Nishida (2008). The ascidian nomenclature system is shown in gray according to Stach et al. (2008) and Nishida and Stach (2014). Developmental fates of cells at 32-cell stage are indicated. CNS, central nervous system

and 9 min later, two polar bodies appear as an obvious signal of successful fertilization (Fig. 4.6) (Fenaux 1998a; Fujii et al. 2008). At 19 °C, the first division takes place after 23 min postfertilization (mpf), generating two morphologically equal cells that correspond to the right and left sides of the animal. At 32 mpf, another symmetric division takes place. This division is meridional and perpendicular to the previous one giving place to the anterior and posterior hemispheres. The third division (at 40 mpf) is asymmetric and leads to the formation of 8 cells, 4 big cells in the animal pole and 4 small cells in the vegetal pole. The morula stage appears 52 mpf, after the fourth division generates an embryo composed of 16 cells. Gastrulation starts 67 mpf, at 32-cell stage, and it consists in the ingression of the vegetal blastomeres that remain covered by the animal blastomeres (Nishida 2008). Neurulation starts at the 64-cell stage 80 mpf, when 8 cells from the anterior region are aligned in two rows of 4 cells that form a matrix that is internalized. Tail bud stage starts 135 mpf, when tail and trunk differentiate. During this stage, the tail elongates, and the embryo bents ventrally. Notochord cells align in a single row and become evident at 180 mpf. At 3.6 h postfertilization (hpf), a larva hatches, and embryogenesis terminates (Fig. 4.6) (Delsman 1910; Cañestro et al. 2005; Fujii et al. 2008; Nishida 2008; Stach et al. 2008).

Larval development is subdivided into six stages (I–VI) (Nishida 2008) that last 6 h at 19 °C, from the hatchling until the juvenile stage (Fig. 4.6). At stage I, the larva elongates and occasionally moves by tail beats. At stage II, the boundaries of the organs begin to appear, and at stage III, the organs are perceptible. At stage IV, organs are clearly recognizable, mouth opens, and the cilia of the digestive system and the ciliary rings of the gill slits start moving. Buccal glands locate at each side of the endostyle, and the heart starts beating. Notochord vacuoles fuse, and the tail flattens to form the lateral fins. At stage V, water current starts inside the larva, the lumen of all organs is continuous, and the trunk epidermis (oikoplasic epithelium) secretes house materials (pre-house). Swimming movements are vigorous. At stage VI, after a few seconds of intense movement, the tail changes its orientation 120° during a process called tailshift (Delsman 1910; Galt and Fenaux 1990; Fenaux 1998b; Nishida 2008). The tailshift event occurs when the larva reaches the juvenile stage, and it is thought comparable to metamorphosis in other urochordates (Fig. 4.6), although in *O. dioica* the definitive organs develop earlier than in ascidian species (Galt and Fenaux 1990).

After the tailshift, juvenile animals inflate the first house and start to feed. During the next days, animals filtrate water and feeds at the time that they grow and their gonads mature. From day 1 to day 3, the trunk grows from 0.17 to 0.35 mm (Bouquet et al. 2009), and the gonad expands in the posterior and ventral part of the trunk to fill the whole posterior region (Fig. 4.5). On day 4, the gonad increases its size becoming wider than the trunk and becomes visible to the unaided eye. At day 5, the trunk of *O. dioica* measures almost 1 mm and the whole animal between 3 and 4 mm (Bouquet et al. 2009). At that time, the gonad is fully developed, and males and females are easily distinguishable as the gonad is full of sperm or eggs, respectively (Figs. 4.5 and 4.6).

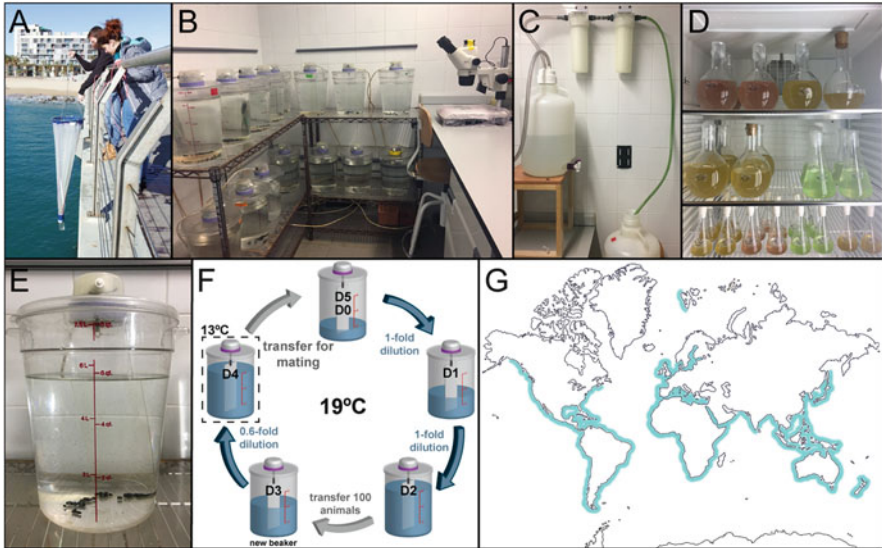


Fig. 4.8 *O. dioica* culture and geographic distribution. Animals might be collected in the coast using a plankton net or directly with a bucket (a) and maintained in the laboratory at 19 °C using a standard air conditioning device (b). Seawater is filtered through 10–0.5 µm polypropylene filters to remove major particles and organisms and sterilized using 0.2 µm filters (c). Three algal species and a cyanobacteria are individually cultured in a 13 °C incubator with a 12 h light/dark photoperiod and used to feed the animals (d). *O. dioica* animals are cultured at 19 °C in polycarbonate backers and maintained in suspension by the rotation (5–15 rpm) of a paddle driven by an electric motor mounted on the lid of the backer (e). A new animal culture starts by mating 20 females and 10 males close to spawn (D0) in a baker with 1.5 L of sterilized seawater (f, top). Next 2 days (D1 and D2), the culture is just diluted adding 1.5 and 3 L of sterilized seawater, respectively (f, right). At day 3 (D3), ≈100 animals are transferred to a new backer with 4 L of fresh sterilized seawater (f, left-down), and at day 4 (D4), cultures are diluted adding 2 L of sterilized seawater and moved to a 13 °C incubator (f, left-top). In the morning of day 5 (D5), most of the animals are mature and ready to set a new mating for new generation (f, top). For additional details, see Martí-Solans et al. (2015). Geographic distribution of the *O. dioica* species in the coast of most of the oceans (blue line) (reviewed in Fenaux et al. 1998, and supplemented with Bary 1960; Fenaux 1972; Costello and Stancyk 1983; Larson 1987; Gaughan and Potter 1994; Hwan Lee et al. 2001; Aravena and Palma 2002; Walkusz et al. 2003; Menéndez et al. 2011) (g)

AU4

357 4.2.3 *O. dioica* Is Easily Accessible, with a Wide Geographic 358 Distribution and Suitable for Lab Culturing

359 4.2.3.1 Geographic Distribution and Abundance

360 *O. dioica* is a semi-cosmopolite free-swimming species present in the Atlantic,
361 Pacific, and Indian Oceans as well as in the Mediterranean and Red Seas, but not
362 in extreme latitude oceans as Arctic or Antarctic (Fenaux et al. 1998) (Fig. 4.8).
363 Although *O. dioica* is a widespread species, its populations may vary in a seasonal
364 way (Essenberg 1922; Raduan et al. 1985; Uye and Ichino 1995; Fenaux et al. 1998;

Tomita et al. 2003). In the west Mediterranean Sea, for instance, its maximum 365 abundance is found during spring and autumn seasons (Raduan et al. 1985). 366 *O. dioica* along with other appendicularian species are so abundant that they occupy 367 an important trophic position in food webs. Appendicularians are the second most 368 abundant species, after copepods, in marine mesozooplankton (Gorsky and Fenaux 369 1998; Captanio et al. 2008), and they graze about 10% of the ocean's primary 370 production (Acuña et al. 2002). Acting as an important short-circuit that allows a 371 rapid energy transfer from colloidal carbon and phytoplankton primary producers to 372 zooplanktivorous predators such as fish larvae (Flood and Deibel 1998; Fernández 373 et al. 2004), they contribute to at least 8% of the vertical carbon transport to the deep 374 ocean (Davoll and Youngbluth 1990; Robison et al. 2005; Troedsson et al. 2013). 375 Appendicularians are, indeed, a major contributor of "marine snow" (i.e., biological 376 debris that originates from the top layers of the ocean and drifts to the seafloor) in 377 euphotic and mesopelagic zones through the production of discarded houses and 378 fecal pellets (Robison et al. 2005). Those particles, full of nutrients, contribute to 379 28–39% of total particulate organic carbon export to the deep oceans (Alldredge 380 2005). The ecological relevance of appendicularians is so high that human activities 381 affecting their populations [e.g., global warming or an increase of toxins in oceans 382 (Bouquet et al. 2018; Torres-Aguila et al. 2018)] might impact on marine food webs 383 and in vertical carbon flux at a world scale. Therefore, the *O. dioica* populations 384 might be valuable sentinels for monitoring marine ecosystems. In summary, 385 *O. dioica* is an ecological relevant organism, abundant in the neritic zone in almost 386 all marine costs, and easily accessible using ordinary plankton nets (Fig. 4.8a, g). 387

4.2.3.2 *O. dioica* Lab Culturing

388

In addition to its accessibility directly from nature, *O. dioica* cultures can be 389 maintained in the laboratory (Fig. 4.8b, f). *O. dioica* was first cultured by 390 Paffenhöfer in 1973, but the bases for a long-term maintenance system were 391 developed by Fenaux and Gorsky (1985). Nowadays, to our knowledge, the pro- 392 cedures to culture *O. dioica* in the laboratory all year around have been published 393 from three facilities in the world located in Norway, Japan, and Spain (our facility) 394 (Nishida 2008; Bouquet et al. 2009; Martí-Solans et al. 2015). We culture the 395 animals at 19 °C in 8 L polycarbonate backers containing 6 L of seawater and 396 10 grams of activated charcoal (see legend of Fig. 4.8 for details). Animals are 397 maintained in suspension by the rotation of a polyvinyl carbonate paddle connected 398 to an electric motor (5–15 rpm). We add 2 or 3 pearls of 1-hexadecanol to reduce 399 surface tension and therefore avoiding that animals get trapped by the surface of the 400 water. For feeding, a cocktail of three different species of algae (*Chaetoceros* 401 *calcitrans*, *Isochrysis* sp., *Rhinomonas reticulata*) and a cyanobacterium 402 (*Synechococcus* sp.) is added to the animal cultures every day. Because growing 403 *O. dioica* specimens can trap only foods of a proper size, the amount of each alga and 404 of the cyanobacterium in the cocktail is adjusted according to their cell sizes along 405 the *O. dioica* life cycle. Animal cultures are a source of mature male and female 406

407 specimens from which developmentally synchronic embryos can be obtained using
408 several in vitro fertilization protocols (Clarke et al. 2007; Martí-Solans et al. 2015;
409 Mikhaleva et al. 2015). Embryos and larvae at different developmental stages can be
410 thereby easily collected, fixed, and stored for experiments on demand.

411 **4.2.4 *O. dioica* Can Be Experimentally Manipulated**

412 **4.2.4.1 Pharmacological Treatments**

413 Pharmacological treatments are a powerful tool to perform functional studies due to
414 its experimental simplicity, and embryos are just transferred to a solution with the
415 drug. The fact that we can easily obtain hundreds of synchronously developing
416 *O. dioica* embryos by in vitro fertilization allows us to perform numerous treatments
417 at different drug concentrations in a fast, simple, and reproducible way. The small
418 size of the *O. dioica* embryos facilitates the diffusion of the drugs to the inner tissues,
419 and their transparency allows the observation of the phenotypic effects of the
420 treatments by DIC microscopy in live developing specimens without the need to
421 perform histological sections. In addition, gene expression responses might be
422 investigated by whole-mount in situ hybridization techniques or by high-density
423 tiling arrays. Pharmacological treatments have been performed, for instance, with
424 developmental morphogens such as all-trans-retinoic acid (RA), which yielded a
425 range of morphological abnormalities, from mild to severe, depending on develop-
426 mental stage, duration, and concentration of RA exposure (Cañestro and
427 Postlethwait 2007). Treatments with xenobiotic compounds such as the carcinogenic
428 polycyclic aromatic hydrocarbon BaP or with the lipid-lowering agent clofibrate
429 have been also assayed to investigate the transcriptional regulation of the xenobiotic
430 defense mechanisms and to identify the *O. dioica* chemical defensesome (Yadatie et al.
431 2012). Finally, treatments with biotoxins such as *trans,trans*-2,4-decadienal, a
432 model for polyunsaturated aldehydes produced during diatom blooms, have been
433 used to analyze the impact on marine food webs of possible future intensification of
434 algal blooms associated with climate change (Torres-Aguila et al. 2018).

435 **4.2.4.2 Techniques for Altering Gene Function by Morpholino, dsRNA, 436 or dsDNA Injections**

437 Different knockdown approaches for altering gene function have been developed in
438 *O. dioica* by injecting morpholinos (Sagane et al. 2010), double-stranded RNA
439 (dsRNA; RNA interference-RNAi) (Omotezako et al. 2013; Mikhaleva et al.
440 2015), or double-stranded DNA (dsDNA; DNA interference-DNAi) (Omotezako
441 et al. 2015, 2017), and new techniques for genome editing based on CRISPR-Cas9
442 are currently being developed (Deng et al. 2018). Most techniques rely on the
443 injection of a given molecule into the gonad of premature females, when it is still

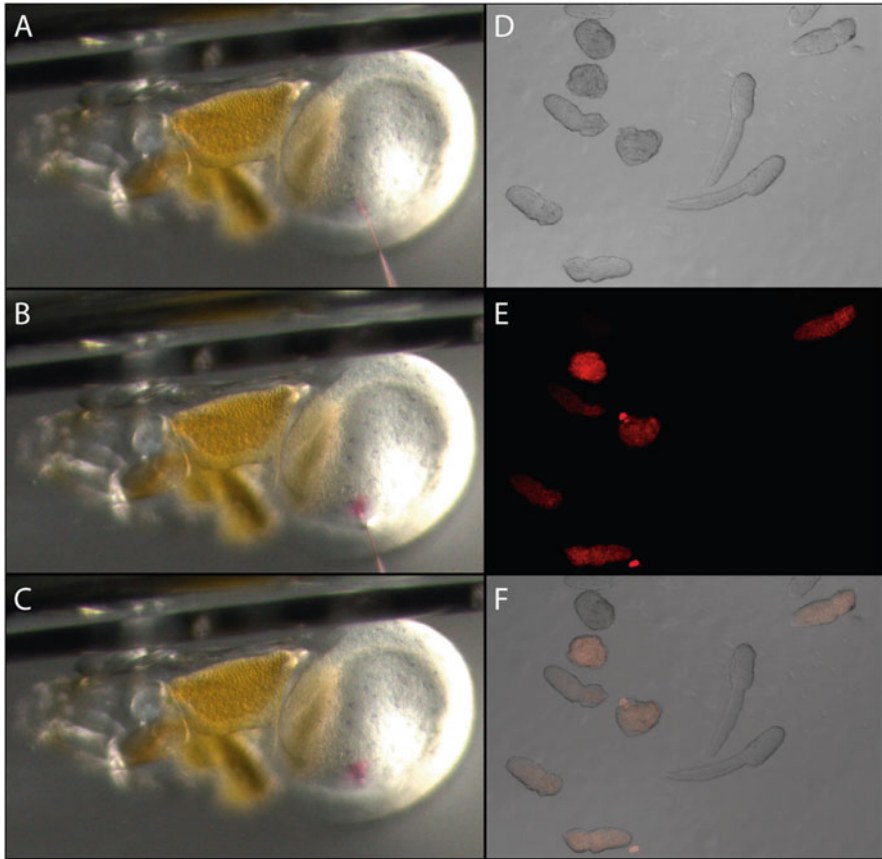


Fig. 4.9 Knocking down by dsDNA injection into the gonad of premature females. A dsDNA against the *brachyury* gene is injected into a premature female gonad (syncytium) (a–c), along with phenol red and *pSD64Flife-act-mCherry-mRNA*. Phenol red allows us to visualize the injected solution (red dot in panels b and c), while mCherry fluorescence highlights the embryos containing mRNA and, therefore, most likely also dsDNA after the cellularization process. In this regard, notice that malformed embryos showing the *brachyury*-dsDNA phenotype are fluorescent (compare panels d–f)

a syncytium of meiotic nuclei surrounded by common cytoplasm (Ganot et al. 2007). 444
 Then, the injected molecule might spread along the forming oocytes, generating tens 445
 of knockdown embryos with a single injection (Fig. 4.9). Alternatively, injections in 446
 spawned eggs are also possible (Mikhaleva et al. 2015, 2018; Deng et al. 2018), 447
 though they are more difficult and less productive. 448

Injection of morpholinos, synthetic molecules of approximately 25 nucleotides in 449
 length that bind to complementary sequences of RNA blocking translation or 450
 altering splicing, was the first knockdown approach in *O. dioica* (Sagane et al. 451
 2010). Morpholinos were used to knock down a cellulose synthase gene necessary 452
 to build the house, obtaining different phenotypes related to the production of 453

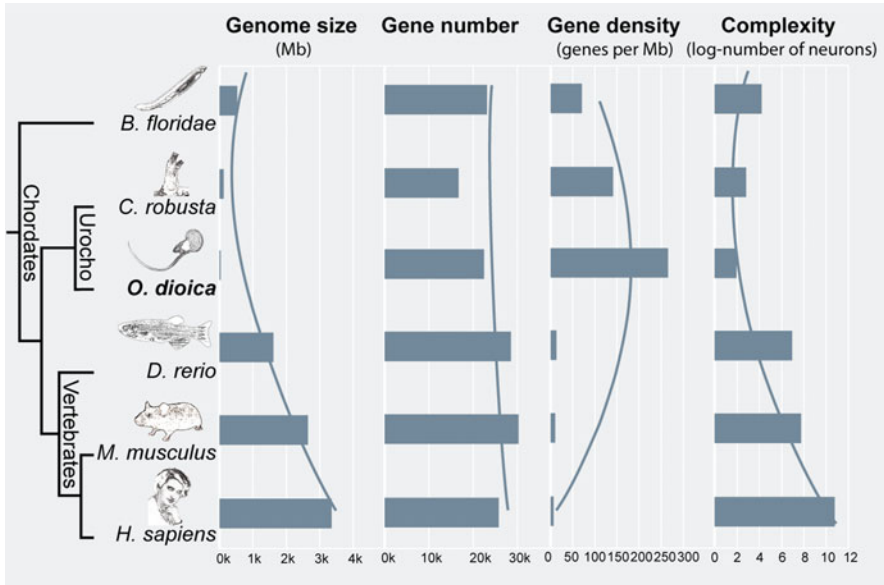


Fig. 4.10 Comparison of genome size, gene number, gene density, and biological complexity among selected chordate species arranged according to their phylogenetic relationships. Bar plots illustrate that *O. dioica* has the smallest chordate genome but has a number of genes rather similar to other chordate species, which implies that *O. dioica* gene density is the highest one. As a rough estimate of biological complexity, we plotted the number of neurons of each organism in logarithmic scale. Lines represent the overall tendency within each plot

454 cellulose fibrils (Sagane et al. 2010). In 2013, RNA interference by dsRNA injection
 455 was used to investigate the development of the tail and the function of the CNS in tail
 456 movement (Omotezako et al. 2013; Mikhaleva et al. 2015). Finally, in 2015, DNA
 457 interference by dsDNA injection, a gene silencing technique reported in plants,
 458 ciliates, and archaea, was successfully assayed in *O. dioica*, being the first case
 459 reported in any metazoan organism (Omotezako et al. 2015). Although the molec-
 460 ular bases for DNAi are unknown, *O. dioica* experiments suggest that dsDNA can
 461 induce sequence-specific transcription blocking and mRNA degradation.

462 **4.2.5 *O. dioica* Occupies a Privileged Phylogenetic Position** 463 **Within the Chordate Phylum**

464 The urochordate (or tunicates), group to which the appendicularian *O. dioica*
 465 belongs, is the sister subphylum of the vertebrates, which together with basally
 466 branching cephalochordates form the chordate phylum (but see Satoh et al. (2014)
 467 for the chordate superphylum hypothesis) (Fig. 4.10). Urochordates are an extremely
 468 diverse taxonomic group that appears to have undergone a rapid evolution and

speciation, spreading over many marine habitats, from shallow waters to deep sea (Holland 2016). Urochordates are classically divided into three classes, Appendicularia (larvaceans, ≈ 70 species including *O. dioica*), Ascidiacea (sea squirts, ≈ 3000 species), and Thaliacea (salps, doliolids, and pyrosomes, ≈ 100 species), although it has been recently proposed that Thaliacea species are nested within the Ascidiacea class (Delsuc et al. 2018; Kocot et al. 2018). In any case, Appendicularians—also known as Larvaceans because they maintain the larval morphology, including the chordate synapomorphies, throughout the entire life cycle—appear to be the sister clade of all other urochordates, representing a branch of the subphylum that split from all other urochordates 450 million years ago (Delsuc et al. 2018). Appendicularians are divided into three families. The Fritillariidae family that includes 3 genera and 30 species, the Kowalevskiidae family, the smallest one with just 1 genus and 2 species, and the Oikopleuridae family, the most diverse group with 11 genera and 37 species (Bone 1998).

O. dioica occupies a privileged phylogenetic position within urochordates for evo-devo studies because it can be morphologically, functionally, genetically, and genomically compared with many other urochordate species (more than 10 ascidians have been totally or partially sequenced; <http://www.aniseed.cnrs.fr/>; <http://octopus.obs-vlfr.fr/public/botryllus/blastbotryllus.php>), including well-studied ascidian species of the *Ciona* or *Halocynthia* genera (Corbo et al. 2001; Dehal et al. 2002; Nishida 2002; Cañestro et al. 2003; Satoh 2003; Satoh et al. 2003; Brozovic et al. 2016, 2017). In addition, from a more general perspective, comparisons of *O. dioica* and ascidians with diverse vertebrate species (there are more than 100 vertebrate genome projects) are relevant for detecting subphylum-specific traits, which might be classified as evolutionary innovations or losses depending on their presence in the external cephalochordate subphylum (there are three *Branchiostoma* genome projects and one *Asymmetron* RNA-Seq project).

4.2.6 *O. dioica* Has Small and Compacted Genome

With only 70 Mb, *O. dioica* genome is the smallest chordate genome and one of the smallest genomes in metazoans (Seo et al. 2001; Denoëud et al. 2010; Danks et al. 2013), only surpassed by the small genomes of some parasite animals (Burke et al. 2015; Chang et al. 2015; Mikhailov et al. 2016) (Table 4.1) (Fig. 4.10). The small size of the *O. dioica* genome is the result of a process of compaction mostly due to three factors: (1) a reduction of the length of intergenic regions, partly because of numerous operons; (2) a reduction of the abundance of transposable elements; and (3) the reduction of the size of introns (Denoëud et al. 2010; Berna and Alvarez-Valin 2014; reviewed in Chavali et al. 2011). As a result of the genome compaction, the gene density in *O. dioica* genome (1 gene per 3.9 kb) has become very high, 3 times higher than in ascidian *C. robusta*, 6 times higher than in cephalochordate amphioxus, and 35 times higher than in human genome (Table 4.1) (Fig. 4.10).

t1.1 **Table 4.1** Main features of *O. dioica* genes and genome (Volff et al. 2004; Denoeud et al. 2010; Chalopin et al. 2015)

t1.2	<i>Genome</i>	
t1.3	Size	70 Mb
t1.4	Size of intergenic regions	53% of intergenic distances <1 kb
t1.5	Population mutation rate	$\theta = 4N_e\mu = 0.0220$
t1.6	Conserved synteny	Negligible
t1.7	Diversity of transposable elements	4 class I retroelements + 3 class II DNA transposons
t1.8	Abundance of transposable elements	10–20% genome (at most few hundreds of each TE)
t1.9	<i>Genes</i>	
t1.10	Number	18,020 predicted genes
t1.11	Density	1 gene per 3.9 kb (257 genes per Mb)
t1.12	Genes in operons	27% (1800 operons)
t1.13	Number of introns per Gene	4.1
t1.14	Intron size	<50 nt in 62% of the genes; >1 kb in 2.4% of the genes
t1.15	Intron position	76% intron positions specie-specific
t1.16	Noncanonical splicing sites	In 12% introns (9% GA-AG, 2.7% GC-AG, 0.7% GG-AG)

509 4.2.6.1 Intergenic Regions and Operons

510 *O. dioica* genes are densely packed, with 53% of their intergenic sequences smaller
 511 than 1 kb (Table 4.1). Contributing to the intragenic reduction, many *O. dioica* genes
 512 are organized in polycistronic transcription units (operons). The majority of operons
 513 are bicistronic (60%), but a substantial proportion contains three or more genes, and
 514 some have up to 11 genes. Operon organization reduces the intergenic space because
 515 it reduces the DNA segments containing transcription initiation and regulation
 516 signals. The fact that 27% of *O. dioica* genes are predicted to be organized in around
 517 1800 operons (Denoeud et al. 2010), together with the observation that most genes
 518 have relatively small intergenic spaces, may favor the genome compaction of this
 519 species (Table 4.1).

520 4.2.6.2 Transposable Elements

521 Transposable elements (TEs or transposons) are main components of eukaryote
 522 genomes that can replicate and change to new locations. *O. dioica* genome is
 523 relatively poor in TEs, in terms of quantity and diversity, and most of the so-called
 524 pan-animal transposon families, many of them even present in *C. robusta* (Cañestro
 525 and Albalat 2012), are absent (Denoeud et al. 2010). *O. dioica* genome contains TEs
 526 of only six superfamilies—*Ty3/Gypsy*, *DIRS1*, and *Penelope*-like retrotransposons
 527 (Volff et al. 2004) and *Tc-Mariner*, *PyggyBac*, and *Maverik* DNA transposons
 528 (Chalopin et al. 2015)—plus a new family of non-LTR retrotransposon named
 529 *Odin* (Volff et al. 2004) (Table 4.1). Although the copy number of each TE is low

(at most few hundreds), LTR retrotransposons appear to be the most abundant (>60%), while non-LTR retrotransposons and DNA transposons represent less than 20% each. The extent of TEs on the *O. dioica* genome size has been estimated about 10–20% (Chalopin et al. 2015). In summary, a massive purge of pan-animal TEs has occurred in *O. dioica* genome probably associated with an intense process of genome compaction. Some TEs show a low level of sequence corruption, suggesting a rather recent activity, but their low copy number and uneven genome distribution indicate that TE expansion in *O. dioica* is under tight genetic control (Denoeud et al. 2010).

4.2.6.3 Introns

Another factor contributing to *O. dioica* genome compaction is the small size of the introns of the majority of the genes (Table 4.1). Despite *O. dioica* having a typical number of introns per gene (4.1) as in other vertebrates, it has reduced the size of the introns to less than 50 nucleotides in 62% of the genes, and only 2.4% of the introns being larger than 1 kb (Seo et al. 2001; Denoeud et al. 2010). *O. dioica* shows a high intron turnover: 76% of the introns are in positions unique to *O. dioica* (newly acquired introns) and only 17% are in ancestral positions (7% remain unclassified) (Denoeud et al. 2010) (Table 4.1). Several mechanisms have been proposed for the gain and loss of introns in *O. dioica* (Denoeud et al. 2010), but since newly acquired introns tend to be shorter than old introns, intron turnover might have favored genome compaction. Surprisingly, canonical splicing signal (GT-AG intron boundaries) is not observed in about 12% of introns (1% in other species), which mostly (9%) have noncanonical GA-AG (GC-AG, 2.7%, or GG-AG, 0.7%) sequences (Edvardsen et al. 2004; Denoeud et al. 2010). Because *O. dioica* lacks the minor spliceosome and only has one type of each spliceosomal component (Denoeud et al. 2010), a single major spliceosome, permissive in terms of splicing signals, would take care of all splicing processes. It has been proposed that such permissive splicing could favor the intron turnover (Denoeud et al. 2010) and, hence, the compaction of the *O. dioica* genome.

4.3 Evolution of *O. dioica* Genes

The *O. dioica* genome project did not only reveal that this species has an extremely compacted genome with small intergenic regions, tiny introns, and few TEs, but that its genes have suffered many evolutionary changes affecting the conservation of the sequence, organization, and number of genes.

564 **4.3.1 Gene Sequence Evolution: High Evolutionary Rates**

565 The sequencing of the genome confirmed that *O. dioica* is a very fast evolver and its
566 genes always show surprisingly long branches in phylogenetic tree reconstructions
567 (Edvardsen et al. 2005; Denoeud et al. 2010). This high rate of sequence evolution
568 appears to be the result of two independent evolutionary forces acting at different
569 levels and with different strength.

570 First, affecting at a global genome scale with a moderate strength, we found that
571 most genes show a high evolutionary rate (Table 4.1) as a result of a combination of
572 a high population mutation rate and a reduced negative (purifying) selection. An
573 estimate of *O. dioica* population mutation rate ($\theta = 4N_e, \mu = 0.0220$) shows it is
574 high, which is consistent with a large effective population size (N_e) and/or a high
575 mutation rate per generation (μ) (Denoeud et al. 2010). In addition, the short
576 generation time of this species implies that the effective mutation rate per year is
577 substantially increased. A reduced negative selection for *O. dioica* has been pro-
578 posed based on the homogeneity of its amino acid rates that is a symptom of
579 relaxation of selective—structural and/or functional—constraints (Berna et al.
580 2012; Berna and Alvarez-Valin 2014). Relaxation of selective constraints associated
581 with rapid rates of sequence evolution has been actually proposed for other fast-
582 evolving animal species such as *Ciona robusta* and *Caenorhabditis elegans* (Hol-
583 land and Gibson-Brown 2003).

584 Second, some particular genes have even a higher evolutionary rate due to
585 positive selection that contributes to the adaptation to new environments or to new
586 challenges (Berna and Alvarez-Valin 2014). Many of these genes with this higher
587 evolutionary rate have been described to be involved in regulatory and developmen-
588 tal functions (Berna et al. 2012; Berna and Alvarez-Valin 2014).

589 **4.3.2 Evolution of Gene and Genome Organization**

590 **4.3.2.1 Negligible Synteny Conservation**

591 Conserved synteny describes the colocalization of homologous genes on homolo-
592 gous chromosomal regions of different species. *O. dioica* genome appears to have
593 suffered numerous chromosomal rearrangements during evolution, and thereby, it
594 lacks any chromosomal synteny conservation with other animal genomes (Denoeud
595 et al. 2010). Conservation of local synteny is also almost negligible since local gene
596 order is indistinguishable from random for distances smaller than 30 genes, and a
597 low level of conserved synteny is only detectable at a wider distance span (Denoeud
598 et al. 2010; Irimia et al. 2012). These observations suggest that constraints that
599 maintain gene order in metazoans may actually be relaxed in *O. dioica*.

4.3.2.2 Disintegration of *Hox* Cluster

600

Another significant feature of *O. dioica* genome is the disintegration of the cluster of *Hox* genes, which is generally well conserved in all bilaterians. *Hox* genes are a subset of homeobox genes involved in establishing morphological identities along the anterior–posterior axis, and although the biological significance of *Hox* clustering remains unclear, functional and structural explanations leading to a spatiotemporal coordinated transcriptional regulation of *Hox* genes have been proposed (Kmita and Duboule 2003). In many species, the position of the *Hox* genes in the cluster correlates with their temporal and spatial sequential expression along the anterior–posterior axis (reviewed in Duboule 2007). *O. dioica* does not have a *Hox* cluster since its complement of nine *Hox* genes—three anterior *Hox* genes (*Hox1*, *Hox2*, and *Hox4*) and six posterior genes (*Hox9A*, *Hox9B*, *Hox10*, *Hox11*, *Hox12*, and *Hox13*)—is totally dispersed in its genome (Seo et al. 2004). The disorganization of the *Hox* cluster in *O. dioica* has been related to the lineage-driven mode of development of *O. dioica*, in which *Hox* genes would contribute to tissue specification with separated domains of *Hox* expressions, rather than to axial patterning with overlapping *Hox* expressions (Seo et al. 2004).

4.3.2.3 Evolution of Operon Organization

617

A third important genomic feature in the organization of *O. dioica* genes is their grouping in operons (Table 4.1). The operons do not only contribute to the compaction of the genome (see above) but might also serve to group genes that have to be either efficiently coregulated—repressing or activating them as a group—or ubiquitously expressed with a low degree of transcriptional regulation (Blumenthal 2004). *O. dioica* has around 1800 operons transcribed as polycistronic pre-mRNAs, most of them processed to mature monocistronic mRNAs via spliced-leader RNA (SL RNA) *trans* splicing (Ganot et al. 2004; Denoëud et al. 2010). Functional annotation of the gene set in operons shows that they are significantly enriched for genes involved in housekeeping functions or general metabolic processes such as RNA, protein, DNA, lipid, and carbohydrate processing and transport. Genes involved in developmental processes such as morphogenesis and organogenesis are, in contrast, significantly underrepresented in the operon gene set (Denoëud et al. 2010).

4.3.3 Gene Number Evolution

632

Despite its reduced size, *O. dioica* genome contains 18,020 predicted genes, a similar number to other urochordates (e.g., *C. robusta* \approx 15,300 genes) and only slightly below other chordates such as the cephalochordate *Branchiostoma floridae*

636 ($\approx 22,000$ genes) or the vertebrate *Fugu rubripes* ($\approx 18,300$ genes) (Table 4.1)
 637 (Fig. 4.10). The current number of genes is the result of the balance between gene
 638 gains and losses impacting a certain set of ancestral genes, and because *O. dioica*
 639 appears to be prone to lose genes (see next section), it has to be also prone to
 640 gain them.

641 Gene duplications have been proposed to be a major driving force for gene gains
 642 (Ohno 1970; Cañestro et al. 2013), and *O. dioica* seems to have retained many
 643 lineage-specific duplicates. For instance, among homeobox genes, *O. dioica* shows a
 644 high incidence of retention of lineage-specific duplicates of genes such as *Irx*, *Not*,
 645 and *Pax3/7* (Edvardsen et al. 2005). Additional examples of such duplicates are
 646 found in g-type lysozyme genes (Nilsen et al. 2003), caspase genes (Weill et al.
 647 2005), metallothionein genes (Calatayud et al. 2018), notochord *Noto15* and *Noto9*
 648 genes (Kugler et al. 2011), *RdhE2* and *Cco* genes (Martí-Solans et al. 2016), and
 649 actin as well as other muscle structural genes (Almazán et al. 2018; Inoue and Satoh
 650 2018), among many others predicted from the genome project analysis (Denoeud
 651 et al. 2010). Lineage-specific duplicates might contribute to both general evolution-
 652 ary adaptations of the organisms and innovations associated with the unique biology
 653 of the lineage. For example, homeobox genes expressed—and possibly patterning—
 654 in the oikoplasic epithelium, which represents a significant novelty of
 655 appendicularians for secreting the mucous house, mostly belong to the duplicated
 656 groups (Denoeud et al. 2010; Mikhaleva et al. 2018), while gene families with cell
 657 adhesion roles are overrepresented in *O. dioica*, most likely because of the extensive
 658 and assorted interactions required for building the house (Chavali et al. 2011).

AU6

659 4.4 Evolution by Gene Loss: *O. dioica* as a Model System 660 for Evo-Devo Studies

661 Urochordate genomes (e.g., *C. robusta*) appear to have a “liberal” evolutionary
 662 pattern of gene loss (Dehal et al. 2002; Holland and Gibson-Brown 2003; Hughes
 663 and Friedman 2005; Somorjai et al. 2018), which contrasts with the “conservative”
 664 pattern of cephalochordates and vertebrates (Somorjai et al. 2018). *O. dioica* appears
 665 to have pushed this urochordate trend to its limits (Ferrier 2011) by having lost many
 666 genes or entire genetic pathways (Table 4.2). In this section, we review these losses
 667 grouped into three categories: Sect. 4.4.1, losses of genes involved in general
 668 characteristics of gene/genomic structure and expression, Sect. 4.4.2, losses of
 669 genes related to particular cellular and physiological functions, and Sect. 4.4.3,
 670 losses of genes essential for embryonic development in chordates.

AU7

Table 4.2 Absent genes^a in *O. dioica* genome

Category	Genes	References	
cNHEJ repair system	<i>Xrcc5 (Ku80), Xrcc6 (Ku70), Xrcc4, Lig4, NHEJ1 (Xlf), DNA-PKc, Dclre1c</i>	Denoeud et al. (2010)	12.1 12.2 12.3
Epigenetic machinery	<i>Dnmt1, Dnmt3, Mbd4/MeCP2, Gcn5/ PcaF, Hat1, Mll1, Ash1, Rnf1, Suz12, Pcgf, Scmh1, kdm2b</i>	Albalat et al. (2012), Navratilova et al. (2017)	12.4
Spliceosome machinery	snRNA U11, snRNA U12, snRNA U4atac, snRNA U6atac	Denoeud et al. (2010)	12.5
Caspase family	<i>Csp1/4/5, Csp6, Csp2/9, Csp8/10</i>	Weill et al. (2005)	12.6
Immune system	<i>NLRs, RLHs, MyD88-like, Sarm1-like, Tirap-like, Ticamp2-like</i>	Denoeud et al. (2010)	12.7
Defense system	<i>AhR, AhRR, Nr1C (Ppar), CYP1 genes</i>	Yadatie et al. (2012)	12.8
Peroxisins	<i>Pex1, Pex2, Pex3, Pex5, Pex6, Pex7, Pex10, Pex11, Pex12, Pex13, Pex14, Pex16, Pex19, Pex26</i>	Zarsky and Tachezy (2015)	12.9
Retinoic acid signaling	<i>Rdh10, Rdh16, Bco1, Aldh1a, Cyp26, RAR, PPAR</i>	Cañestro et al. (2006), Cañestro and Postlethwait (2007), Martí-Solans et al. (2016)	12.10
Homeobox genes	<i>Hox3, Hox5, Hox6, Hox7, Hox8, Gbx, Nk3, Nk6, TGIF, POU VI, Lhx6/7, Vax, Cux, SATB, ZFH1, Sax, Xlox, Mox, Hlx, Bsh, Chox10, Otp, Prx, goosecoid, Prox, Tlx</i>	Seo et al. (2004), Edvardsen et al. (2005)	12.11
Sox genes	<i>SoxC, SoxE, SoxF, SoxH</i>	Heenan et al. (2016)	12.12
miRNA	miR-9, miR-29, miR-33, miR-34, miR-96, miR-126, miR-133, miR-135, miR-153, miR-182, miR-183, miR-184, miR-196, miR-200, miR-216, miR-217, miR-218, miR-367	Wang et al. (2017)	12.13
Notochord genes	<i>Entactin, fibrinogen-like, multidom, myomegalin, Noto1, Noto2, Noto3, Noto4, Noto5, Noto6, Noto7, Noto8, Noto11, Noto12, Noto13, Noto14, Noto16, perlecan, Ptp, Slc, Swipi, tropomyosin-like, tune, Ube2</i>	Kugler et al. (2011)	12.14
General repair system	<i>Polb, Apex2, Lig3, Msh3, Atm, Chek2, Aptx, Nbn, Rad52</i>	Denoeud et al. (2010)	12.15
Apoptotic genes	<i>Bax, Bak, BCL-X_L</i>	Robinson et al. (2012)	12.16
Cyclins and CDK	<i>Cyclin J, cyclin G, cyclin F, Cdk14/15</i>	Campsteijn et al. (2012)	12.17
Rab GTPases	<i>Rab4, Rab7L1, Rab9, Rab15, Rab19/43, Rab20, Rab21, Rab22, Rab24, Rab26/37, Rab28, Rab30, Rab32LO, Rab40, Ift27, Rasef, EFCab44/Rab44, RabX1, RabX4, RabX6</i>	Coppola et al. (2019)	12.18

^aGenes are not found in *O. dioica*, and, thereby, are likely lost during the evolution of the *O. dioica* lineage

671 **4.4.1 Loss of Genes Involved in Gene/Genomic Structure**
 672 **and Expression**

673 **4.4.1.1 Loss of Non-homologous End Joining Repair Genes**

674 All organisms have the ability to repair the double-strand breaks (DSBs) that
 675 normally happen in DNA due to numerous external and internal factors. One
 676 fundamental mechanism present in all eukaryotes to repair these breaks is the
 677 canonical non-homologous end joining (cNHEJ) repair system. Unexpectedly,
 678 *O. dioica* (Denoeud et al. 2010) and other six species of appendicularians (Deng
 679 et al. 2018; Ferrier and Sogabe 2018) do not have the cNHEJ machinery (Table 4.2),
 680 meaning this repair system became dispensable during the evolution of this chordate
 681 lineage. In fact, *O. dioica* seems to use the alternative NHEJ (aNHEJ) system
 682 (a.k.a. alternative end joining, aEJ, Pannunzio et al. 2018) as a compensatory system
 683 that overcomes DSBs, although the existence of another so far undescribed pathway
 684 cannot be excluded (Deng et al. 2018). Because the aNHEJ system seems to be less
 685 faithful than cNHEJ (it often involves deletion of some intervening nucleotides and
 686 commonly leads to chromosome rearrangements, for example, translocations,
 687 (Deriano and Roth 2013)), the loss of the cNHEJ system might have had important
 688 consequences in the genome architecture. It may have contributed, for instance, to
 689 the compaction of the *O. dioica* genome by either favoring the deletions caused by
 690 the aNHEJ repair system or by restricting replication of autonomous
 691 retrotransposons that uses the cNHEJ system for their propagation (Deng et al.
 692 2018). In addition, this loss may have also contributed to the reorganization of the
 693 genome through accumulated rearrangements, leading to negligible synteny conser-
 694 vation (Deng et al. 2018) that may be associated with modifications of the mecha-
 695 nisms of gene regulation, changing from long-range mechanisms acting on
 696 topologically associated genomic blocks that include several genes to short-range
 697 and gene-specific systems for gene regulation (Cañestro et al. 2007; Ferrier and
 698 Sogabe 2018).

AU8

699 **4.4.1.2 Loss of Genes of the Epigenetic Machinery**

700 Histone modifications and DNA methylation are epigenetic marks mainly associated
 701 with regulation of gene expression, replication, DNA repair, recombination, chro-
 702 mosome segregation, and other meiotic and mitotic processes. Histone proteins,
 703 responsible of packing DNA into nucleosomes, provide multiple sites for posttrans-
 704 lational modifications by evolutionarily conserved histone modifiers that establish
 705 the so-called histone code. Among the proteins that modify histones, *O. dioica* has
 706 lost several genes for histone acetyltransferases such as *Gcn5/Pcaf* and *Hat1*
 707 (Navratilova et al. 2017) (Table 4.2). In addition, homologs of core components of
 708 the canonical Polycomb complexes (*Rnf1*, *Suz12*, *Pcgf*, and *Scmh1*) and genes for
 709 several proteins of the trithorax group (*Mll1*, *Ash1*, and *Kdm2b*) have neither been

found in *O. dioica*'s genome (Navratilova et al. 2017). Regarding DNA methylation, *O. dioica* has lost the two main DNA methyltransferases *Dnmt1* and *Dnmt3*, and one of the two *Mbd* genes, *Mbd4/MeCP2* (Cañestro et al. 2007; Albalat et al. 2012) (Table 4.2). Overall, it is through that the loss of components of the epigenetic machinery might have favored changes in the genome architecture and modifications of the mechanisms of gene regulation, leading to compacted regulatory spaces, reduced chromatin state domain widths, evolution of operons, and loss of synteny and dispersion of the Hox cluster (Cañestro et al. 2007; Navratilova et al. 2017).

4.4.1.3 Loss of Minor Spliceosome Genes

While the major spliceosome containing the snRNAs U1, U2, U4, U5, and U6 removes introns with canonical GT-AG boundaries, the minor spliceosome, which contains the snRNAs U11, U12, U4atac, U5, and U6atac, mainly acts on noncanonical AT-AC boundaries (Patel and Steitz 2003; Sheth et al. 2006). Both major and minor spliceosomes are present across most eukaryotic lineages tracing them back to the origin of eukaryote evolution. Although *O. dioica* has many noncanonical introns (see above), no AT-AC introns have been detected in cDNA resources (Denoeud et al. 2010), which may explain that none of the minor splicing snRNAs are found in *O. dioica* (Table 4.2). It seems therefore that in the absence of AT-AC introns, the components of the minor spliceosome became dispensable and lost during *O. dioica* evolution and at the same time that the major spliceosome became permissive and able to remove all—canonical and noncanonical—*O. dioica* introns, although with different efficiency (Denoeud et al. 2010). Whether these differences in splicing efficiency could reflect specific usage of noncanonical introns for gene expression regulation and what evolutionary impact these changes had needs further investigation.

4.4.2 Loss of Genes for Cellular and Physiological Functions

4.4.2.1 Loss of Genes of the Caspase Family

Caspases are a family of protease enzymes that play an important role not only in apoptosis but also in maturation of different immunity system proteins and in the control of the proliferation and differentiation of specific cell types (Weill et al. 2005). Caspases are present in all kingdoms (Uren et al. 2000), but their number has a taxon-dependent diversity ranging from 3 members in *C. elegans* to 10–13 in vertebrates and 17 in *C. robusta* (Weill et al. 2005). *O. dioica* has only three caspase genes deriving from a single founder distantly related to *Caspase 3/7* (Weill et al. 2005) (Table 4.2). *O. dioica* seems, therefore, to have lost all of the components of the caspase family except one. The reduced complexity of the caspase family might be associated with a low cell number at the adult stage, the absence of a major

747 metamorphosis event, and a minimized immune system in this species (Weill et al.
748 2005).

749 4.4.2.2 Loss of Genes of the Immune System

750 As a marine organism, *O. dioica* should have an innate immune system prepared to
751 fight against viruses and bacteria present in high amounts in seawater, but its short
752 life span along with the absence of hemolymph cells—hemocytes or macrophages—
753 points to a rapid immune system based on transcriptional upregulation response or
754 on constitutively expressed effectors, rather than to a more slow system reliant on
755 cell proliferation triggered by immune receptors (Denoeud et al. 2010). In agree-
756 ment, *O. dioica* has lost almost all genes with domains corresponding to typical
757 immune receptors or immune effectors and lacks homologous genes to interleukins
758 or cytokines involved in the immunity response of more complex chordates
759 (Denoeud et al. 2010) (Table 4.2). Interestingly, it has been proposed that a simpli-
760 fied immune system may be compensated by the antibacterial function of some
761 oikosins with phospholipase A2 domains, which hydrolyze glycerophospholipids
762 present in bacterial cell walls (Hosp et al. 2012). In summary, *O. dioica* seems to
763 have a highly derived and simplified strategy of defense that together with its high
764 fertility, short life cycle, and high polymorphism contributes to the survival of the
765 *O. dioica* populations (Denoeud et al. 2010).

766 4.4.2.3 Loss of Cyp Genes for Xenobiotic Defensome Systems

767 The first step for elimination or inactivation of xenobiotic compounds often involves
768 the oxidative modification of the toxic chemicals, mostly performed by enzymes of
769 the cytochrome P450 (CYP) family, some of which are also required for embryonic
770 development (Goldstone et al. 2006). Due to its variable functions, Cyp enzymes are
771 quite abundant in animal genomes—up to 120 *Cyp* genes in sea urchin (Goldstone
772 et al. 2006), 94 in zebrafish (Goldstone et al. 2010), or 236 in amphioxus (Nelson
773 et al. 2013). *O. dioica*, however, has lost many *Cyp* genes, and with only 23 *Cyp*
774 genes, this species has the smallest *Cyp* repertoire among sequenced metazoan
775 genomes (Yadatie et al. 2012). *O. dioica* lacks, for instance, the CYP1 family
776 genes, which play a central role in the metabolism of environmental toxicants
777 (Table 4.2). *O. dioica* also lacks the aryl hydrocarbon receptor (*AhR*) gene (and its
778 repressor *AhRR*) (Yadatie et al. 2012), which is the transcriptional regulator of CYP1
779 family genes and a major xenobiotic sensing receptor activated by pollutants.
780 Overall, these data suggest the absence of an AhR-mediated xenobiotic biotransforma-
781 tion signaling pathway in *O. dioica* and suggest the evolution of alternative
782 mechanisms of response to environmental xenobiotic compounds (Yadatie et al.
783 2012).

4.4.2.4 Loss of Peroxin Genes and Absence of Peroxisomes

784

Peroxisomes are single membrane-bound organelles with important functions in detoxification of reactive oxygen species, long-chain fatty acid beta-oxidation, plasmalogen synthesis, amino acid degradation, and purine metabolism. Peroxisome biosynthesis and protein import is mediated by a group of 13 highly conserved eukaryotic proteins called peroxins (Gabaldon et al. 2006; Schluter et al. 2006; Zarsky and Tachezy 2015). Peroxisomes are ubiquitous in eukaryotes, and only some groups of anaerobic protist and parasitic helminths lack peroxisomes (Schluter et al. 2006; Gabaldon and Capella-Gutierrez 2010). It is therefore extraordinary that *O. dioica* has lost all peroxin genes (Table 4.2), becoming the only known aerobic non-parasitic organism that does not have peroxisomes (Zarsky and Tachezy 2015). The evolutionary and physiological conditions in which *O. dioica* was able to lose the peroxisomes are still a matter of debate as this organism has high oxygen consumption and oxidizes fatty acids for ATP synthesis, unlike the anaerobic parasitic lineages missing these organelles (Zarsky and Tachezy 2015). It has been proposed that the loss of peroxisomes might be evolutionary adaptive, since it has been associated with reduced genomes and traits of r-reproductive strategies such as high fecundity, early maturation, and simplified ontogenesis, which *O. dioica* shares with parasite organisms as well as with some selective advantages by rendering organisms resistant to xenobiotics that become activated in the peroxisomal lumen by redox reactions (Zarsky and Tachezy 2015).

4.4.3 Loss of Genes Essential for Embryonic Development in Chordates

805

806

4.4.3.1 Loss of the RA Genetic Machinery

807

All-*trans*-RA is a vitamin A-derived compound that acts as a crucial signaling system involved in the differentiation and outgrowth of neurons in many metazoans (reviewed in Albalat 2009), which was adopted for Hox-controlled anterior–posterior patterning in the chordate phylum (Handberg-Thorsager et al. 2018). Despite the crucial role of RA in chordate axial patterning, it has been shown that *O. dioica* has lost most of the genes for RA production, degradation, and signaling (i.e., the RA genetic machinery, including *Rdh10*, *Aldh1a*, *Cyp26*, and *RAR* genes) (Cañestro et al. 2006, 2007; Cañestro and Postlethwait 2007; Martí-Solans et al. 2016) (Table 4.2) (Fig. 4.11). In the absence of mutational robustness (i.e., alternative pathways) capable of compensating them, these gene losses were accompanied by the loss of the RA signaling in this species (Martí-Solans et al. 2016).

The loss of the RA genetic machinery in *O. dioica* probably took place in the context of regressive evolution associated with the disintegration of the Hox cluster that, as mentioned in Sect. 4.3.2, has been related with the shift to a determinative mode of development. This shift would have released the restrictions to maintain the



Fig. 4.11 The loss of the retinoic acid genetic machinery in *O. dioica* exemplifies how functionally linked genes are co-eliminated during evolution. In the absence of mutational robustness capable of compensating the loss, the co-elimination was accompanied by the loss of the RA signaling. *O. dioica* has lost genes for the Rdh10, Rdh16, Bco1, Aldh1a, and Cyp26 enzymes, as well as genes for the RAR and PPAR nuclear receptors (strikethrough in lighter boxes). The surviving genes (i.e., *Adh1/4*, *RdhE2*, *Aldh8a1*, and *Cco* in dark boxes) (Cañestro et al. 2010; Martí-Solans et al. 2016) do not constitute an alternative pathway for RA synthesis because neither RA nor RA precursors have been detected at concentrations that are likely to play any role in developmental or physiological processes of this species (strikethrough)

823 integrity of the Hox cluster (Seo et al. 2004) and led extracellular signals such as RA
 824 that establish embryonic coordinates and regulate the expression of *Hox* genes by
 825 gradually increasing the portion of the cluster exposed to transcription machinery
 826 over time to become dispensable and eventually lost (Cañestro and Postlethwait
 827 2007; Cañestro et al. 2007).

828 4.4.3.2 Loss of Homeobox Gene Families

829 Homeobox genes encode transcription factors involved in many developmental
 830 processes in eukaryotes. Homeobox genes are classified into 11 classes and over
 831 100 gene families/groups (Holland et al. 2007), some of them vertebrate innovations.
 832 *O. dioica* has lost 36 homeobox groups, 12 of which probably lost during the early
 833 urochordate evolution and 14 specifically lost in the *O. dioica* lineage (Edvardsen
 834 et al. 2005) (Table 4.2). Noteworthy, among the homeobox families, *O. dioica* has
 835 lost the anterior *Hox3* and all the central *Hox* genes of the cluster (Seo et al. 2004). In
 836 parallel with the losses, homeobox genes have also duplicated during the evolution
 837 of *O. dioica* lineage (Edvardsen et al. 2005). Interpreting these gains and losses in
 838 terms of the evolution of developmental mechanisms remains difficult until the
 839 function of *O. dioica* homeobox genes is revealed. It has been proposed that family
 840 losses may be the result of a relaxed selective pressure to conserve the full set of
 841 homeobox families in the *O. dioica* (or in the urochordate) lineage due to a
 842 simplification of its body plan in comparison with that of the chordate ancestor
 843 (Edvardsen et al. 2005). On the other hand, the preservation of duplicates in some

families might be the result of a re-diversification of homeobox genes after major group losses (Edvardsen et al. 2005). 844 845

4.4.3.3 Loss of *Sox* Genes 846

Sox (Sry-type HMG box) genes are a family of transcription factors defined by a conserved sequence called the high-mobility group (HMG) box. *Sox* genes are involved in a number of essential functions during embryonic development, including sex determination and neuronal development (Wegner 2010). Ten different *Sox* groups have been described (A to J), some of them (B, C, D, E, F) conserved in almost all metazoans, and some groups being specific of certain lineages (A, G, and I of vertebrates, H of chordates, and J of nematodes) (Bowles et al. 2000; Heenan et al. 2016). *O. dioica*, however, has only four *Sox* genes, two of them belonging to the *SoxD* group and the other two to the *SoxB* group (Heenan et al. 2016; Torres-Aguila et al. 2018). These results imply that *O. dioica* has lost three ancient metazoan *Sox* groups (C, E, F) and the chordate *Sox* group (H) (Heenan et al. 2016) (Table 4.2). As in other examples reviewed above, the evolutionary impact of the gains and losses in the *Sox* family on the developmental mechanisms remains difficult to interpret since the expression of only two *SoxB* genes has been described (Torres-Aguila et al. 2018). 847 848 849 850 851 852 853 854 855 856 857 858 859 860 861

4.4.3.4 Loss of miRNAs 862

MicroRNAs (miRNAs) are noncoding RNAs of about 22 nucleotides involved in the regulation of different biological processes, including embryo development, cell differentiation, and growth. miRNA innovation has been correlated with increased developmental complexity during animal evolution (Hertel et al. 2006). Analysis of the miRNA repertoire of *O. dioica* has shown that this species has lost (or derived to the point they cannot be recognized anymore) at least eighteen highly conserved bilaterian miRNA families (Fu et al. 2008; Wang et al. 2017) (Table 4.2). On the other hand, at least 29 new miRNA families would have appeared in appendicularians (Fu et al. 2008), suggesting a profound reorganization of the miRNA repertoire due to recurrent events of gene losses and gains during *O. dioica* evolution. This scenario is consistent with the general notion that animal miRNAs are poorly conserved between distant taxa (Wang et al. 2017) and, therefore, that changes in miRNA repertoires have been important in shaping animal evolution (Fu et al. 2008). It is thought that the reorganization of *O. dioica* miRNA repertoire might have impacted on the temporal robustness of the rapid developmental program of this urochordate lineage (Fu et al. 2008), which would be in agreement with the idea that modifications in the miRNA repertoires have been important in adapting radically different life-history strategies from a common larval body plan (Fu et al. 2008). 863 864 865 866 867 868 869 870 871 872 873 874 875 876 877 878 879 880 881

882 4.4.3.5 Loss of Notochord Genes

883 The notochord, one of defining features of the chordate phylum, is a stiff rod of
884 tissue located ventral to the neural tube that provides a rigid, but still bendy, structure
885 for muscle attachment, as well as an important source of embryonic developmental
886 signals (Stemple 2005). Actually, developing chordate embryos require a notochord
887 as an organizer for secreting signals that pattern several organs such as the somites,
888 heart, or pancreas. Comparison of a set of notochord genes known to be targets of the
889 notochord-specific Brachyury transcription factor revealed that from 50 notochord
890 genes of *C. robusta* used as a reference, 24 are absent in *O. dioica* (likely lost, e.g.,
891 *Noto2*), and 15 are not expressed (8 genes, e.g., *Asak*) or expressed at low levels
892 (7 genes, e.g., *Noto10*) in the notochord (Kugler et al. 2011) (Table 4.2). Taken
893 together, these results suggest a considerable divergence in the genetic toolkit for
894 notochord development in *O. dioica*, which it would have been impacted by events
895 of gene loss or by the loss of the notochord function of some genes. Considering the
896 morphological similarities between urochordate notochords, the divergence in the
897 genetic toolkits used to develop them is surprising.

898 4.4.4 *O. dioica*, Gene Loss, and the Inverse Paradox

899 The original paradox in the field of evo-devo arose by the discovery that similar
900 genetic toolkits were able to build a wide variety of morphologies in disparate
901 animals, implying that the same genes (genetic unity) were used to build such
902 different forms (phenotypic diversity) (Jacob 1977). The discovery of the pervasive-
903 ness of gene loss along evolution (Albalat and Cañestro 2016) affecting relevant
904 developmental genes led to the formulation of the so-called inverse paradox of
905 evo-devo. This hypothesis proposes that organisms might develop fundamentally
906 similar morphologies (phenotypic unity) despite important differences in their
907 genetic toolkits (genetic diversity) (Cañestro et al. 2007) (Fig. 4.12). Because
908 differences between the genetic toolkits are often a consequence of the loss of
909 some of their crucial genes, the study of *O. dioica* has become fundamental to
910 build the new conceptual framework as this species has been able to maintain a
911 phylotypic chordate-body plan after having lost many genes thought to be crucial for
912 the archetypal chordate development (see Sect. 4.4.3). In this regard, the character-
913 ization of the *O. dioica* “lossosome” (the complete catalogue of gene losses in a
914 phylogenetic context; Cañestro and Roncalli 2018) and the analysis of its functional
915 consequences should provide the framework to investigate how gene loss might
916 have been an important evolutionary force for generating differences in the devel-
917 opmental genetic toolkits of chordates and, thereby, to understand the evolution of
918 the mechanisms of development of our own phylum.

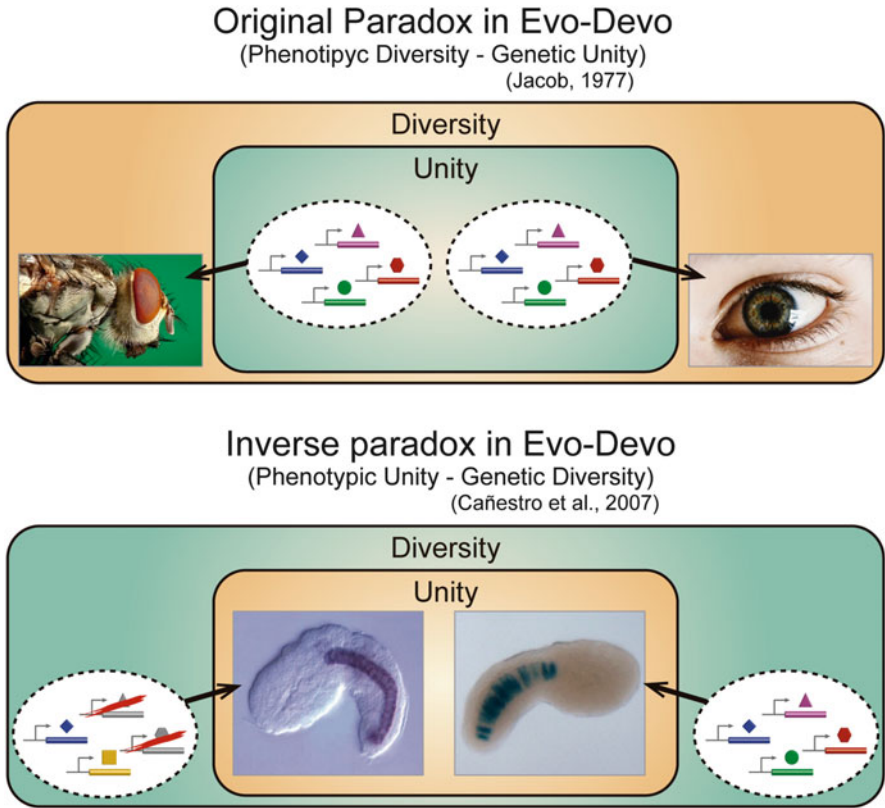


Fig. 4.12 In contrast to the original paradox, the inverse paradox in evo-devo proposes that organisms might develop fundamentally similar morphologies (phenotypic unity) despite important differences in their genetic toolkits (genetic diversity). Because differences in the genetic toolkits often are the consequence of the gene losses, the study of *O. dioica* has been fundamental to build this new conceptual framework

4.5 Future Directions

919

The tiny planktonic chordate *Oikopleura dioica* appears as an emerging nonclassical 920 animal model, not only attractive to better understand the radiation of our own 921 phylum in the field of evo-devo but also attractive in many other biological fields, 922 such as ecology, environmental toxicology, biomedicine, or basic research. In 923 ecology and toxicology, for instance, the relevance of *O. dioica* and other larvacean 924 species in the marine food webs makes the study of its defense and detoxification 925 mechanisms significant for understanding the impact of industrial pollutants or the 926 effect of the climate change on marine environments, trophic webs, and ocean 927 production. Monitoring *O. dioica* populations has been proposed to be used as 928 valuable sentinels for following the health of marine ecosystems and the expression 929 of its defense genes as molecular biosensors that marine biologists could use to 930

931 monitor stress situations of natural populations. For biomedical applications, the
 932 chordate condition of *O. dioica* makes it closer to humans than classical model
 933 animals such as fruit flies or worms, but genetically and functionally more tractable
 934 than classical vertebrate models as mouse or zebrafish. The homology of organs,
 935 tissues, and structures between *O. dioica* and vertebrates (i.e., human) is unquestionable
 936 and therefore a good proxy to understand the genetic bases of many human
 937 disorders. In addition, the genetic, functional, and structural similarities of *O. dioica*
 938 and vertebrates make this species a promising model system for pharmacological
 939 screenings and other functional tests by amenable knockdown systems such as RNAi
 940 or DNAi approaches. Moreover, the relative small and compact genome of *O. dioica*
 941 makes it a good system for basic research in genetics. In the field of gene regulation
 942 analysis, for example, its small intergenic regions should facilitate the identification
 943 of *cis*-regulatory elements that control gene transcription. And in the field of
 944 evolutionary biology, the high mutation rate of *O. dioica*, its propensity to lose
 945 genes, and its miniature genome that can be affordably sequenced in many individuals
 946 should facilitate studies of population genomics for better understanding evolutionary
 947 forces in natural populations, searching for adaptive interpopulation
 948 differences, or investigating microevolution processes. Thus, *O. dioica* research
 949 has a brilliant present, but an even more promising future.

950 **Acknowledgments** The authors thank all current and former members of the C.C. and
 951 R.A. laboratories for fruitful scientific discussions on evolution, gene loss, and *Oikopleura dioica*.
 952 We thank Annamaria Locascio for the *Ciona robusta* picture. C.C. was supported by BFU2016-
 953 80601-P grant, and R.A. was supported by BIO2015-67358-C2-1-P grant from Ministerio de
 954 Economía y Competitividad (Spain). C.C. and R.A. were also supported by grant SGR2017-1665
 955 from Generalitat de Catalunya. A.F-R. was supported by a FPU14/02654 fellowship from
 956 Ministerio de Educación Cultura y Deporte.

957 References

- 958 Acuña JL, Kiefer M (2000) Functional response of the appendicularian *Oikopleura dioica*. *Limnol*
 959 *Oceanogr* 45:608–618
- 960 Acuña JL, Bedo AW, Harris RP, Anadón R (1995) The seasonal succession of appendicularians
 961 (Tunicata: Appendicularia) off Plymouth. *J Mar Biol Assoc UK* 75:755–758
- 962 Acuña JL, Deibel D, Saunders P, Booth B, Hatfield E, Klein B, Mei ZP, Rivkin R (2002)
 963 Phytoplankton ingestion by appendicularians in the North Water. *Deep Sea Res Part II Top*
 964 *Stud Oceanogr* 49:5101–5115
- 965 Albalat R (2009) The retinoic acid machinery in invertebrates: ancestral elements and vertebrate
 966 innovations. *Mol Cell Endocrinol* 313:23–35
- 967 Albalat R, Cañestro C (2016) Evolution by gene loss. *Nat Rev Genet* 17:379–391
- 968 Albalat R, Martí-Solans J, Cañestro C (2012) DNA methylation in amphioxus: from ancestral
 969 functions to new roles in vertebrates. *Brief Funct Genomics* 11:142–155
- 970 Allredge AL (2005) The contribution of discarded appendicularian houses to the flux of particulate
 971 organic carbon from oceanic surface waters. In: Gorsky G, Youngbluth MJ, Deibel D (eds)
 972 Response of marine ecosystems to global change: ecological impact of appendicularians.
 973 Éditions Scientifiques, Paris

- Almazán A, Ferrández-Roldán A, Albalat R, Cañestro C (2018) Developmental atlas of appendicularian *Oikopleura dioica* actins provides new insights into the evolution of the notochord and the cardio-paraxial muscle in chordates. *Dev Biol*. <https://doi.org/10.1016/j.ydbio.2018.09.003>
- Aravena GP, Palma S (2002) Taxonomic identification of appendicularians collected in the epipelagic waters off northern Chile (Tunicata, Appendicularia). *Rev Chilena Hist Nat* 75:307–325
- Bary BM (1960) Notes on ecology, distribution, and systematics of Pelagic Tunicata from New Zealand. *Pac Sci* 14(2):101–121
- Bassham S, Postlethwait J (2000) Brachyury (T) expression in embryos of a larvacean urochordate, *Oikopleura dioica*, and the ancestral role of T. *Dev Biol* 220:322–332
- Bedo AW, Acuña JL, Robins D, Harris RP (1993) Grazing in the micron and the sub-micron particle size range: the case of *Oikopleura dioica* (Appendicularia). *Bull Mar Sci* 52:2–14
- Berna L, Alvarez-Valin F (2014) Evolutionary genomics of fast evolving tunicates. *Genome Biol Evol* 6:1724–1738
- Berna L, D'Onofrio G, Alvarez-Valin F (2012) Peculiar patterns of amino acid substitution and conservation in the fast evolving tunicate *Oikopleura dioica*. *Mol Phylogenet Evol* 62:708–717
- Blumenthal T (2004) Operons in eukaryotes. *Brief Funct Genomic Proteomic* 3:199–211
- Bollner T, Holmberg K, Olsson R (1986) A rostral sensory mechanism in *Oikopleura dioica* (Appendicularia). *Acta Zool (Stockholm)* 67:235–241
- Bone Q (1998) The biology of pelagic tunicates. Oxford University Press, New York
- Bone Q, Mackie GO (1975) Skin impulses and locomotion in *Oikopleura* (tunicata: larvacea). *Biol Bull* 149:267–286
- Bouquet JM, Spriet E, Troedsson C, Ottera H, Chourrout D, Thompson EM (2009) Culture optimization for the emergent zooplanktonic model organism *Oikopleura dioica*. *J Plankton Res* 31:359–370
- Bouquet JM, Troedsson C, Novac A, Reeve M, Lechtenborger AK, Massart W, Skaar KS, Aasjord A, Dupont S, Thompson EM (2018) Increased fitness of a key appendicularian zooplankton species under warmer, acidified seawater conditions. *PLoS One* 13:e0190625
- Bowles J, Schepers G, Koopman P (2000) Phylogeny of the SOX family of developmental transcription factors based on sequence and structural indicators. *Dev Biol* 227:239–255
- Brozovic M, Martin C, Dantec C, Dauga D, Mendez M, Simion P, Percher M, Laporte B, Scornavacca C, Di Gregorio A, Fujiwara S, Gineste M, Lowe EK, Piette J, Racioppi C, Ristoratore F, Sasakura Y, Takatori N, Brown TC, Delsuc F, Douzery E, Gissi C, Mcdougall A, Nishida H, Sawada H, Swalla BJ, Yasuo H, Lemaire P (2016) ANISEED 2015: a digital framework for the comparative developmental biology of ascidians. *Nucleic Acids Res* 44:D808–D818
- Brozovic M, Dantec C, Dardaillon J, Dauga D, Faure E, Gineste M, Louis A, Naville M, Nitta KR, Piette J, Reeves W, Scornavacca C, Simion P, Vincentelli R, Bellec M, Aicha SB, Fagotto M, Gueroult-Bellone M, Haussler M, Jacox E, Lowe EK, Mendez M, Roberge A, Stolfi A, Yokomori R, Brown CT, Cambillau C, Christiaen L, Delsuc F, Douzery E, Dumollard R, Kusakabe T, Nakai K, Nishida H, Satou Y, Swalla B, Veeman M, Volf JN, Lemaire P (2017) ANISEED 2017: extending the integrated ascidian database to the exploration and evolutionary comparison of genome-scale datasets. *Nucleic Acids Res* 46:D718–D725
- Burighel P, Brena C (2001) Gut ultrastructure of the appendicularian *Oikopleura dioica* (Tunicata). *Invertebr Biol* 120:278–293
- Burke M, Scholl EH, Bird DM, Schaff JE, Colman SD, Crowell R, Diener S, Gordon O, Graham S, Wang X, Windham E, Wright GM, Opperman CH (2015) The plant parasite *Pratylenchus coffeae* carries a minimal nematode genome. *Nematology* 17:621
- Calatayud S, Garcia-Risco M, Rojas NS, Espinosa-Sanchez L, Artime S, Palacios O, Cañestro C, Albalat R (2018) Metallothioneins of the urochordate *Oikopleura dioica* have Cys-rich tandem repeats, large size and cadmium-binding preference. *Metallomics* 10:1585–1594

- 1026 Campsteijn C, Ovrebø JI, Karlsen BO, Thompson EM (2012) Expansion of cyclin D and CDK1
1027 paralogs in *Oikopleura dioica*, a chordate employing diverse cell cycle variants. *Mol Biol Evol*
1028 29:487–502
- 1029 Cañestro C, Albalat R (2012) Transposon diversity is higher in amphioxus than in vertebrates:
1030 functional and evolutionary inferences. *Brief Funct Genomics* 11:131–141
- 1031 Cañestro C, Postlethwait JH (2007) Development of a chordate anterior-posterior axis without
1032 classical retinoic acid signaling. *Dev Biol* 305:522–538
- 1033 Cañestro C, Roncalli V (2018) Gene losses did not stop the evolution of big brains. *elife* 7:e41912
- 1034 Cañestro C, Bassham S, Postlethwait JH (2003) Seeing chordate evolution through the *Ciona*
1035 genome sequence. *Genome Biol* 4:208–211
- 1036 Cañestro C, Bassham S, Postlethwait JH (2005) Development of the central nervous system in the
1037 larvacean *Oikopleura dioica* and the evolution of the chordate brain. *Dev Biol* 285:298–315
- 1038 Cañestro C, Postlethwait JH, Gonzalez-Duarte R, Albalat R (2006) Is retinoic acid genetic machin-
1039 ery a chordate innovation? *Evol Dev* 8:394–406
- 1040 Cañestro C, Yokoi H, Postlethwait JH (2007) Evolutionary developmental biology and genomics.
1041 *Nat Rev Genet* 8:932–942
- 1042 Cañestro C, Bassham S, Postlethwait JH (2008) Evolution of the thyroid: Anterior-posterior
1043 regionalization of the *Oikopleura* endostyle revealed by *Otx*, *Pax 2/5/8*, and *Hox1* expression.
1044 *Dev Dyn* 237:1490–1499
- 1045 Cañestro C, Albalat R, Postlethwait JH (2010) *Oikopleura dioica* alcohol dehydrogenase class
1046 3 provides new insights into the evolution of retinoic acid synthesis in chordates. *Zool Sci*
1047 27:128–133
- 1048 Cañestro C, Albalat R, Irimia M, Garcia-Fernandez J (2013) Impact of gene gains, losses and
1049 duplication modes on the origin and diversification of vertebrates. *Semin Cell Dev Biol*
1050 24:83–94
- 1051 Captanio FL, Curelovich J, Tresguerres M, Negri RM, Viñas MD, Esnal GB (2008) Seasonal cycle
1052 of appendicularians at a coastal station (38°28'S, 57°41'W) of the SW Atlantic Ocean. *Bull Mar*
1053 *Sci* 82:171–184
- 1054 Chalopin D, Naville M, Plard F, Galiana D, Volff JN (2015) Comparative analysis of transposable
1055 elements highlights mobilome diversity and evolution in vertebrates. *Genome Biol Evol*
1056 7:567–580
- 1057 Chang ES, Neuhof M, Rubinstein ND, Diamant A, Philippe H, Huchon D, Cartwright P (2015)
1058 Genomic insights into the evolutionary origin of Myxozoa within Cnidaria. *Proc Natl Acad Sci*
1059 *USA* 112:14912–14917
- 1060 Chavali S, Morais DA, Gough J, Babu MM (2011) Evolution of eukaryotic genome architecture:
1061 insights from the study of a rapidly evolving metazoan, *Oikopleura dioica*: non-adaptive forces
1062 such as elevated mutation rates may influence the evolution of genome architecture. *BioEssays*
1063 33:592–601
- 1064 Cima F, Brena C, Burighel P (2002) Multifarious activities of gut epithelium in an appendicularian
1065 (*Oikopleura dioica*: Tunicata). *Mar Biol* 141:479–490
- 1066 Clarke T, Bouquet JM, Fu X, Kallsoe T, Schmid M, Thompson EM (2007) Rapidly evolving
1067 lamins in a chordate, *Oikopleura dioica*, with unusual nuclear architecture. *Gene* 396:159–169
- 1068 Cleaver O, Krieg PA (2001) Notochord patterning of the endoderm. *Dev Biol* 234:1–12
- 1069 Coppola U, Ristoratore F, Albalat R, D'aniello S (2019) The evolutionary landscape of the Rab
1070 family in chordates. *Cell Mol Life Sci* (In press)
- 1071 Corbo JC, Di Gregorio A, Levine M (2001) The ascidian as a model organism in developmental and
1072 evolutionary biology. *Cell* 106:535–538
- 1073 Costello J, Stancyk SE (1983) Tidal influence upon appendicularian abundance in North Inlet
1074 estuary, South Carolina. *J Plankton Res* 5:263–277
- 1075 Danks G, Campsteijn C, Parida M, Butcher S, Doddapaneni H, Fu B, Petrin R, Metpally R,
1076 Lenhard B, Wincker P, Chourrout D, Thompson EM, Manak JR (2013) OikoBase: a genomics
1077 and developmental transcriptomics resource for the urochordate *Oikopleura dioica*. *Nucleic*
1078 *Acids Res* 41:D845–D853

Davoll P, Youngbluth M (1990) Heterotrophic activity on appendicularian (Tunicata: Appendicularia) houses in mesopelagic regions and their potential contribution to particle flux. *Deep-Sea Res* 37:285–294 1079–1081

Dehal P, Satou Y, Campbell RK, Chapman J, Degnan B, De Tomoso A, Davidson B, Di Gregorio A, Gelpke M, Goodstein DM, Harafuji N, Hastings KEM, Ho I, Hotta K, Huang W, Kawashima T, Lemaire P, Martinez D, Meinertzhagen IA, Necula S, Nonaka M, Putnam N, Rash S, Saiga H, Satake M, Terry A, Yamada L, Wang H-G, Awazu S, Azumi K, Boore J, Branno M, Chin-Bow S, Desantis R, Doyle S, Francino P, Keys DN, Haga S, Hayashi H, Hino K, Imai KS, Inaba K, Kano S, Kobayashi K, Kobayashi M, Lee B-I, Makabe KW, Manohar C, Matassi G, Medina M, Mochizuki Y, Mount S, Morishita T, Miura S, Nakayama A, Nishizaka S, Nomoto H, Ohta F, Oishi K, Rigoutsos I, Sano M, Sasaki A, Sasakura Y, Shoguchi E, Shin-I T, Spagnuolo A, Stainier D, Suzuki MM, Tassy O, Takatori N, Tokuoka M, Yagi K, Yoshizaki F, Wada S, Zhang C, Hyatt PD, Larimer F, Detter C, Doggett N, Glavina T, Hawkins T, Richardson P, Lucas S, Kohara Y, Levine M, Satoh N, Rokhsar DS (2002) The draft genome of *Ciona intestinalis*: insights into chordate and vertebrate origins. *Science* 298:2157–2167 1093–1094

Delsman HC (1910) Beiträge zur Entwicklungsgeschichte von *Oikopleura dioica*. *Verh Rijksinst Onderz Zee* 3:1–24 1095–1096

Delsman HC (1912) Weitere beobachtungen über die entwicklung von *Oikopleura dioica*. *Tijdschr ned dierk Ver* 12:199–206 1097–1098

Delsuc F, Philippe H, Tsagkogeorga G, Simion P, Tilak MK, Turon X, Lopez-Legentil S, Piette J, Lemaire P, Douzery EJP (2018) A phylogenomic framework and timescale for comparative studies of tunicates. *BMC Biol* 16:39 1100–1101

Deng W, Henriot S, Chourrout D (2018) Prevalence of mutation-prone microhomology-mediated end joining in a chordate lacking the c-NHEJ DNA repair pathway. *Curr Biol* 28(3337–3341): e3334 1102–1104

Denooud F, Henriot S, Mungpakdee S, Aury JM, Da Silva C, Brinkmann H, Mikhaleva J, Olsen LC, Jubin C, Cañestro C, Bouquet JM, Danks G, Poulain J, Campsteijn C, Adamski M, Cross I, Yadetie F, Muffato M, Louis A, Butcher S, Tsagkogeorga G, Konrad A, Singh S, Jensen MF, Cong EH, Eikeseth-Otteraa H, Noel B, Anthouard V, Porcel BM, Kachouri-Lafond R, Nishino A, Ugolini M, Chourrout P, Nishida H, Aasland R, Huzurbazar S, Westhof E, Delsuc F, Lehrach H, Reinhardt R, Weissenbach J, Roy SW, Artiguenave F, Postlethwait JH, Manak JR, Thompson EM, Jaillon O, Du Pasquier L, Boudinot P, Liberles DA, Volff JN, Philippe H, Lenhard B, Roest Crollius H, Wincker P, Chourrout D (2010) Plasticity of animal genome architecture unmasked by rapid evolution of a pelagic tunicate. *Science* 330:1381–1385 1109–1113

Deriano L, Roth DB (2013) Modernizing the nonhomologous end-joining repertoire: alternative and classical NHEJ share the stage. *Annu Rev Genet* 47:433–455 1114–1115

Duboule D (2007) The rise and fall of Hox gene clusters. *Development* 134:2549–2560 1116

Edvardsen RB, Lerat E, Maeland AD, Flat M, Tewari R, Jensen MF, Lehrach H, Reinhardt R, Seo HC, Chourrout D (2004) Hypervariable and highly divergent intron-exon organizations in the chordate *Oikopleura dioica*. *J Mol Evol* 59:448–457 1117–1119

Edvardsen RB, Seo HC, Jensen MF, Mialon A, Mikhaleva J, Bjordal M, Cartry J, Reinhardt R, Weissenbach J, Wincker P, Chourrout D (2005) Remodelling of the homeobox gene complement in the tunicate *Oikopleura dioica*. *Curr Biol* 15:R12–R13 1120–1122

Essenberg CE (1922) The seasonal distribution of the Appendicularia in the region of San Diego, California. *Ecology* 3:55–64 1123–1124

Fenaux R (1972) A historical survey of the appendicularians from the area covered by the IIOE. *Mar Biol* 16:230–235 1125–1126

Fenaux R (1976) Cycle vital d'un appendiculaire: *Oikopleura dioica* Fol, 1872. *Ann Inst Océanogr Paris* 52:89–101 1127–1128

Fenaux R (1986) The house of *Oikopleura dioica* (Tunicata, Appendicularia): structure and functions. *Zoomorphology* 106:224–231 1129–1130

- 1131 Fenaux R (1998a) Anatomy and functional morphology of the Appendicularia. In: Bone Q (ed) The
 1132 biology of pelagic tunicates. Oxford University Press, New York
- 1133 Fenaux R (1998b) Life history of the Appendicularia. In: Bone Q (ed) The biology of pelagic
 1134 tunicates. Oxford University Press, Oxford
- 1135 Fenaux R, Gorsky G (1985) Nouvelle technique d'élevage des appendiculaires. Rapp Comm Int
 1136 Mer Médit 29:291–292
- 1137 Fenaux R, Bone Q, Deibel D (1998) Appendicularian distribution and zoogeography. In: Bone Q
 1138 (ed) The biology of pelagic tunicates. Oxford University Press, Oxford
- 1139 Fernández D, López-Urrutia A, Fernández A, Acuña JL, Harris R (2004) Retention efficiency of 0.2
 1140 to 6 µm particles by the appendicularians *Oikopleura dioica* and *Friillaria borealis*. Mar Ecol
 1141 Prog Ser 266:89–101
- 1142 Ferrier DE (2011) Tunicates push the limits of animal evo-devo. BMC Biol 9:3
- 1143 Ferrier DEK, Sogabe S (2018) Genome biology: unconventional DNA repair in an extreme
 1144 genome. Curr Biol 28:R1208–R1210
- 1145 Flood PR, Afzelius BA (1978) The spermatozoon of *Oikopleura dioica* Fol (Larvacea, Tunicata).
 1146 Cell Tissue Res 191:27–37
- 1147 Flood PR, Deibel D (1998) The appendicularian house. In: Bone Q (ed) The biology of pelagic
 1148 tunicates. Oxford University Press, Oxford
- 1149 Fol H (1872) Etudes sur les Appendiculaires du Déroit de Messine. Mem Soc Physique Hist Nat
 1150 Geneve 21:445
- 1151 Fredriksson G, Olsson R (1981) The oral gland cells of *Oikopleura dioica* (Tunicata
 1152 Appendicularia). Acta Zool (Stockholm) 62:195–200
- 1153 Fredriksson G, Olsson R (1991) The subchordal cells of *Oikopleura dioica* and *Oikopleura*
 1154 *albicans* (Appendicularia, Chordata). Acta Zool (Stockholm) 72:251–256
- 1155 Fredriksson G, Ofverholm T, Ericson LE (1985) Ultrastructural demonstration of iodine binding
 1156 and peroxidase activity in the endostyle of *Oikopleura dioica* (Appendicularia). Gen Comp
 1157 Endocrinol 58:319–327
- 1158 Fu X, Adamski M, Thompson EM (2008) Altered miRNA repertoire in the simplified chordate,
 1159 *Oikopleura dioica*. Mol Biol Evol 25:1067–1080
- 1160 Fujii S, Nishio T, Nishida H (2008) Cleavage pattern, gastrulation, and neurulation in the
 1161 appendicularian, *Oikopleura dioica*. Dev Genes Evol 218:69–79
- 1162 Gabaldon T, Capella-Gutierrez S (2010) Lack of phylogenetic support for a supposed
 1163 actinobacterial origin of peroxisomes. Gene 465:61–65
- 1164 Gabaldon T, Snel B, Van Zimmeren F, Hemrika W, Tabak H, Huynen MA (2006) Origin and
 1165 evolution of the peroxisomal proteome. Biol Direct 1:8
- 1166 Galt CP (1972) Development of *Oikopleura dioica* (Urochordata: Larvacea): ontogeny of behavior
 1167 and of organ systems related to construction and use of the house. PhD, University of
 1168 Washington, Seattle
- 1169 Galt C (1978) Bioluminescence: dual mechanism in a planktonic tunicate produces brilliant surface
 1170 display. Science 200:70–72
- 1171 Galt CP, Fenaux R (1990) Urochordata larvacea. In: Adiyodi KG, Adiyodi RG (eds) Reproductive
 1172 biology of invertebrates. Oxford and IBH, New Delhi
- 1173 Ganot P, Kallesoe T, Reinhardt R, Chourrout D, Thompson EM (2004) Spliced-leader RNA trans
 1174 splicing in a chordate, *Oikopleura dioica*, with a compact genome. Mol Cell Biol 24:7795–7805
- 1175 Ganot P, Bouquet JM, Kallesoe T, Thompson EM (2007) The *Oikopleura* coenocyst, a unique
 1176 chordate germ cell permitting rapid, extensive modulation of oocyte production. Dev Biol
 1177 302:591–600
- 1178 Gaughan D, Potter IC (1994) Relative abundance and seasonal changes in the macrozooplankton of
 1179 the lower estuary in South-Western Australia. Rec West Aust Mus 16:461–474
- 1180 Georges D, Holmberg K, Olsson R (1988) The ventral midbrain cells in *Oikopleura dioica*
 1181 (Appendicularia). Acta Embryol Morphol Exp 9:39–47
- 1182 Goldschmidt R (1903) Notiz über die Entwickelung der Appendicularien-Biologisches
 1183 Centralblatt, Band

Goldstone JV, Hamdoun A, Cole BJ, Howard-Ashby M, Nebert DW, Scally M, Dean M, Epel D, Hahn ME, Stegeman JJ (2006) The chemical defensible: environmental sensing and response genes in the *Strongylocentrotus purpuratus* genome. *Dev Biol* 300:366–384 1184–1186

Goldstone JV, McArthur AG, Kubota A, Zanette J, Parente T, Jonsson ME, Nelson DR, Stegeman JJ (2010) Identification and developmental expression of the full complement of Cytochrome P450 genes in Zebrafish. *BMC Genomics* 11:643 1187–1189

Gorsky G, Fenaux R (1998) The role of Appendicularia in marine food webs. In: Bone Q (ed) *The biology of pelagic tunicates*. Oxford University Press, Oxford 1190–1191

Gorsky G, Fisher N, Fowler S (1984) Biogenic debris from the pelagic tunicate *Oikopleura dioica* and its role in the vertical transport of a transuranium element. *Est Coast Shelf Sci* 18:13–23 1192–1193

Handberg-Thorsager M, Gutierrez-Mazariegos J, Arold ST, Kumar Nadendla E, Bertucci PY, Germain P, Tomancak P, Pierzchalski K, Jones JW, Albalat R, Kane MA, Bourguet W, Laudet V, Arendt D, Schubert M (2018) The ancestral retinoic acid receptor was a low-affinity sensor triggering neuronal differentiation. *Sci Adv* 4:eaa01261 1194–1196

Heenan P, Zondag L, Wilson MJ (2016) Evolution of the Sox gene family within the chordate phylum. *Gene* 575:385–392 1197–1199

Hertel J, Lindemeyer M, Missal K, Fried C, Tanzer A, Flamm C, Hofacker IL, Stadler PF, Students of Bioinformatics Computer Labs A (2006) The expansion of the metazoan microRNA repertoire. *BMC Genomics* 7:25 1200–1202

Holland LZ (2016) Tunicates. *Curr Biol* 26:R146–R152 1203

Holland LZ, Gibson-Brown J (2003) The *Ciona intestinalis* genome: when the constraints are off. *BioEssays* 25:529–532 1204–1205

Holland L, Gorsky G, Fenaux R (1988) Fertilization in *Oikopleura dioica* (Tunicata, Appendicularia): acrosome reaction, cortical reaction and sperm-egg fusion. *Zoomorphology* 108:229–243 1206–1208

Holland PW, Booth HA, Bruford EA (2007) Classification and nomenclature of all human homeobox genes. *BMC Biol* 5:47 1209–1210

Holmberg K (1982) The ciliated brain duct of *Oikopleura dioica* (Tunicata, Appendicularia). *Acta Zool* 63:101–109 1211–1212

Holmberg K (1984) A transmission electron microscopic investigation of the sensory vesicle in the brain of *Oikopleura dioica* (Appendicularia). *Zoomorphology* 104:298–303 1213–1214

Hopcroft RR, Roff JC (1995) Zooplankton growth rates: extraordinary production by the larvacean *Oikopleura dioica* in tropical waters. *J Plankton Res* 17:205–220 1215–1216

Hopcroft RR, Roff JC, Bouman HA (1998) Zooplankton growth rates: the larvaceans *Appendicularia*, *Fritillaria* and *Oikopleura* in tropical waters. *J Plankton Res* 20:539–555 1217–1218

Hosp J, Sagane Y, Danks G, Thompson EM (2012) The evolving proteome of a complex extracellular matrix, the *Oikopleura* house. *PLoS One* 7:e40172 1219–1220

Hughes AL, Friedman R (2005) Loss of ancestral genes in the genomic evolution of *Ciona intestinalis*. *Evol Dev* 7:196–200 1221–1222

Hwan Lee J, Chae J, Kim W-R, Won Jung S, Man Kim J (2001) Seasonal variation of phytoplankton and zooplankton communities in the Coastal Waters off Tongyeong in Korea. *Ocean Polar Res* 23:245–253 1223–1225

Inoue J, Satoh N (2018) Deuterostome genomics: lineage-specific protein expansions that enabled chordate muscle evolution. *Mol Biol Evol* 35:914–924 1226–1227

Irimia M, Tena JJ, Alexis MS, Fernandez-Minan A, Maeso I, Bogdanovic O, De La Calle-Mustienes E, Roy SW, Gomez-Skarmeta JL, Fraser HB (2012) Extensive conservation of ancient microsynteny across metazoans due to cis-regulatory constraints. *Genome Res* 22:2356–2367 1228–1231

Jacob F (1977) Evolution and tinkering. *Science* 196:1161–1166 1232

Kimura S, Ohshima C, Hirose E, Nishikawa J, Itoh T (2001) Cellulose in the house of the appendicularian *Oikopleura rufescens*. *Protoplasma* 216:71–74 1233–1234

King KR, Hollibaugh JT, Azam F (1980) Predator-prey interactions between the larvacean *Oikopleura dioica* and bacterioplankton in enclosed water columns. *Mar Biol* 56:49–57 1235–1236

- 1237 Kishi K, Onuma TA, Nishida H (2014) Long-distance cell migration during larval development in
1238 the appendicularian, *Oikopleura dioica*. *Dev Biol* 395:299–306
- 1239 Kishi K, Hayashi M, Onuma TA, Nishida H (2017) Patterning and morphogenesis of the intricate
1240 but stereotyped oikoplasmic epidermis of the appendicularian, *Oikopleura dioica*. *Dev Biol*
1241 428:245–257
- 1242 Kmita M, Duboule D (2003) Organizing axes in time and space; 25 years of colinear tinkering.
1243 *Science* 301:331–333
- 1244 Kocot KM, Tassia MG, Halanych KM, Swalla BJ (2018) Phylogenomics offers resolution of major
1245 tunicate relationships. *Mol Phylogenet Evol* 121:166–173
- 1246 Kugler JE, Kerner P, Bouquet JM, Jiang D, Di Gregorio A (2011) Evolutionary changes in the
1247 notochord genetic toolkit: a comparative analysis of notochord genes in the ascidian *Ciona* and
1248 the larvacean *Oikopleura*. *BMC Evol Biol* 11:21
- 1249 Kusakabe T, Araki I, Satoh N, Jeffery WR (1997) Evolution of chordate actin genes: evidence from
1250 genomic organization and amino acid sequences. *J Mol Evol* 44:289–298
- 1251 Larson RJ (1987) Daily ration and predation by medusae and ctenophores in Saanich Inlet, B.C.,
1252 Canada. *Neth J Sea Res* 21:35–44
- 1253 Last JM (1972) Egg development, fecundity and growth of *Oikopleura Dioica* Fol in the North Sea.
1254 *ICES J Mar Sci* 34:232–237
- 1255 Lohmann H (1933) Erste Klasse der Tunicaten: Appendiculariae. In: Kükenthal W, Krumbach T
1256 (eds) *Handbuch der Zoologie*. Walter De Gruyter, Berlin
- 1257 Lopez-Urrutia A, Acuña JL (1999) Gut throughput dynamics in the appendicularian *Oikopleura*
1258 *dioica*. *Mar Ecol Prog Ser* 191:195–205
- 1259 Martinucci G, Brena C, Cima F, Burighel P (2005) Synchronous spermatogenesis in
1260 appendicularians. In: Gorsky G, Youngbluth M, Deibel D (eds) *Response of marine ecosystems*
1261 *to global changes: ecological impact of appendicularians*. Éditions des Archives
1262 Contempaines, Paris
- 1263 Martí-Solans J, Ferrández-Roldán A, Godoy-Marín H, Badia-Ramentol J, Torres-Aguila NP,
1264 Rodríguez-Marí A, Bouquet JM, Chourrout D, Thompson EM, Albalat R, Cañestro C (2015)
1265 *Oikopleura dioica* culturing made easy: a low-cost facility for an emerging animal model in
1266 *EvoDevo*. *Genesis* 53:183–193
- 1267 Martí-Solans J, Belyaeva OV, Torres-Aguila NP, Kedishvili NY, Albalat R, Cañestro C (2016)
1268 Coelimination and survival in gene network evolution: dismantling the RA-signaling in a
1269 chordate. *Mol Biol Evol* 33:2401–2416
- 1270 Menéndez M, Biancalana F, Berasategui A, Fernández Severini MD, Hoffmeyer MS, Esteves JL
1271 (2011) Mesozooplankton composition and spatial distribution, Nuevo Gulf, Patagonia, Argenti-
1272 na. *Check List* 7:101–107
- 1273 Mikhailov KV, Slyusarev GS, Nikitin MA, Logacheva MD, Penin AA, Aleoshin VV, Panchin YV
1274 (2016) The genome of *Intoshia linei* affirms orthonectids as highly simplified spiralian. *Curr*
1275 *Biol* 26:1768–1774
- 1276 Mikhaleva Y, Kreneisz O, Olsen LC, Glover JC, Chourrout D (2015) Modification of the larval
1277 swimming behavior in *Oikopleura dioica*, a chordate with a miniaturized central nervous system
1278 by dsRNA injection into fertilized eggs. *J Exp Zool B Mol Dev Evol*
- 1279 Mikhaleva Y, Skinnis R, Sumic S, Thompson EM, Chourrout D (2018) Development of the house
1280 secreting epithelium, a major innovation of tunicate larvaceans, involves multiple homeodomain
1281 transcription factors. *Dev Biol* 443:117–126
- 1282 Nakamura Y, Suzuki K, Suzuki S, Hiromi J (1997) Production of *Oikopleura dioica*
1283 (Appendicularia) following a picoplankton ‘bloom’ in a eutrophic coastal area. *J Plankton*
1284 *Res* 19:113–124
- 1285 Navratilova P, Danks GB, Long A, Butcher S, Manak JR, Thompson EM (2017) Sex-specific
1286 chromatin landscapes in an ultra-compact chordate genome. *Epigenetics Chromatin* 10:3
- 1287 Nelson DR, Goldstone JV, Stegeman JJ (2013) The cytochrome P450 genesis locus: the origin and
1288 evolution of animal cytochrome P450s. *Philos Trans R Soc Lond Ser B Biol Sci* 368:20120474

Nilsen IW, Myrnes B, Edvardsen RB, Chourrout D (2003) Urochordates carry multiple genes for goose-type lysozyme and no genes for chicken- or invertebrate-type lysozymes. <i>Cell Mol Life Sci</i> 60:2210–2218	1289 1290 1291
Nishida H (1987) Cell lineage analysis in ascidian embryos by intracellular injection of a tracer enzyme. III Up to the tissue restricted stage. <i>Dev Biol</i> 121:526–541	1292 1293
Nishida H (2002) Patterning the marginal zone of early ascidian embryos: localized maternal mRNA and inductive interactions. <i>BioEssays</i> 24:613–624	1294 1295
Nishida H (2008) Development of the appendicularian <i>Oikopleura dioica</i> : culture, genome, and cell lineages. <i>Develop Growth Differ</i> 50(Suppl 1):S239–S256	1296 1297
Nishida H, Stach T (2014) Cell lineages and fate maps in tunicates: conservation and modification. <i>Zool Sci</i> 31:645–652	1298 1299
Nishino A, Morisawa M (1998) Rapid oocyte growth and artificial fertilization of the Larvaceans <i>Oikopleura dioica</i> and <i>Oikopleura longicauda</i> . <i>Zool Sci</i> 15:723–727	1300 1301
Nishino A, Satoh N (2001) The simple tail of chordates: phylogenetic significance of appendicularians. <i>Genesis</i> 29:36–45	1302 1303
Nishino A, Satou Y, Morisawa M, Satoh N (2000) Muscle actin genes and muscle cells in the appendicularian, <i>Oikopleura longicauda</i> : phylogenetic relationships among muscle tissues in the urochordates. <i>J Exp Zool</i> 288:135–150	1304 1305 1306
Ohno S (1970) <i>Evolution by gene duplication</i> . Springer, New York	1307
Olsson R (1963) Endostyles and endostylar secretions: a comparative histochemical study. <i>Acta Zool (Stockholm)</i> 44:299–329	1308 1309
Olsson R (1965a) Comparative morphology and physiology of the <i>Oikopleura</i> notochord. <i>Isr J Zool</i> 14:213–220	1310 1311
Olsson R (1965b) The cytology of the endostyle of <i>Oikopleura dioica</i> . <i>Ann NY Acad Sci</i> 118:1038–1051	1312 1313
Olsson R (1975) Primitive coronet cells in the brain of <i>Oikopleura</i> (Appendicularia, Tunicata). <i>Acta Zool (Stockholm)</i> 56:155–161	1314 1315
Olsson R, Holmberg K, Lilliemark Y (1990) Fine structure of the brain and brain nerves of <i>Oikopleura dioica</i> (Urochordata, Appendicularia). <i>Zool Morphol</i> 110:1–7	1316 1317
Omotezako T, Nishino A, Onuma TA, Nishida H (2013) RNA interference in the appendicularian <i>Oikopleura dioica</i> reveals the function of the Brachyury gene. <i>Dev Genes Evol</i> 223:261–267	1318 1319
Omotezako T, Onuma TA, Nishida H (2015) DNA interference: DNA-induced gene silencing in the appendicularian <i>Oikopleura dioica</i> . <i>Proc Biol Sci</i> 282:20150435	1320 1321
Omotezako T, Matsuo M, Onuma TA, Nishida H (2017) DNA interference-mediated screening of maternal factors in the chordate <i>Oikopleura dioica</i> . <i>Sci Rep</i> 7:44226	1322 1323
Onuma TA, Isobe M, Nishida H (2017) Internal and external morphology of adults of the appendicularian, <i>Oikopleura dioica</i> : an SEM study. <i>Cell Tissue Res</i> 367:213–227	1324 1325
Paffenhöfer G-A (1973) The cultivation of an appendicularian through numerous generations. <i>Mar Biol</i> 22:183–185	1326 1327
Pannunzio NR, Watanabe G, Lieber MR (2018) Nonhomologous DNA end-joining for repair of DNA double-strand breaks. <i>J Biol Chem</i> 293:10512–10523	1328 1329
Patel AA, Steitz JA (2003) Splicing double: insights from the second spliceosome. <i>Nat Rev Mol Cell Biol</i> 4:960–970	1330 1331
Raduan A, Blanco C, Soler E, Del Rio JG, Raga JA (1985) The seasonal distribution of the Appendicularia in the Bay of Cullera, Spain. <i>Rapp Comm Int Mer Médit</i> 29:293–294	1332 1333
Robinson AJ, Kunji ER, Gross A (2012) Mitochondrial carrier homolog 2 (MTCH2): the recruitment and evolution of a mitochondrial carrier protein to a critical player in apoptosis. <i>Exp Cell Res</i> 318:1316–1323	1334 1335 1336
Robison BH, Reisenbichler KR, Sherlock RE (2005) Giant larvacean houses: rapid carbon transport to the deep sea floor. <i>Science</i> 308:1609–1611	1337 1338
Sagane Y, Zech K, Bouquet JM, Schmid M, Bal U, Thompson EM (2010) Functional specialization of cellulose synthase genes of prokaryotic origin in chordate larvaceans. <i>Development</i> 137:1483–1492	1339 1340 1341

- 1342 Salensky W (1903) Etudes anatomiques sur les Appendiculaires. I *Oikopleura vanhoeffeni*
 1343 Lohmann. Mem Acad Sci St Petesbourg Ser 13:1–44
- 1344 Salensky W (1904) Etudes anatomiques sur les Appendiculaires. II *Oikopleura refescens*. Fol Mem
 1345 Acad Sci St Petesbourg Ser 15:1–54
- 1346 Salensky W (1905) Zur Morphologie der Cardialorgane der Appendicularien. Sixième Congrès
 1347 International de Zoologie, Berne. Kandiget fils. Genève, 381–383
- 1348 Sato R, Tanaka Y, Ishimaru T (2003) Species-specific house productivity of appendicularians. Mar
 1349 Ecol Prog Ser 259:163–172
- 1350 Satoh N (2003) The ascidian tadpole larva: comparative molecular development and genomics. Nat
 1351 Rev Genet 4:285–295
- 1352 Satoh N, Satou Y, Davidson B, Levine M (2003) *Ciona intestinalis*: an emerging model for whole-
 1353 genome analyses. Trends Genet 19:376–381
- 1354 Satoh N, Tagawa K, Takahashi H (2012) How was the notochord born? Evol Dev 14:56–75
- 1355 Satoh N, Rokhsar D, Nishikawa T (2014) Chordate evolution and the three-phylum system. Proc
 1356 Biol Sci 281:20141729
- 1357 Schluter A, Fourcade S, Ripp R, Mandel JL, Poch O, Pujol A (2006) The evolutionary origin of
 1358 peroxisomes: an ER-peroxisome connection. Mol Biol Evol 23:838–845
- 1359 Seo H-C, Kube M, Edvardsen RB, Jensen MF, Beck A, Spriet E, Gorsky G, Thompson EM,
 1360 Lehrach H, Reinhardt R, Chourrout D (2001) Miniature genome in the marine chordate
 1361 *Oikopleura dioica*. Science 294:2506
- 1362 Seo HC, Edvardsen RB, Maeland AD, Bjordal M, Jensen MF, Hansen A, Flaot M, Weissenbach J,
 1363 Lehrach H, Wincker P, Reinhardt R, Chourrout D (2004) Hox cluster disintegration with
 1364 persistent anteroposterior order of expression in *Oikopleura dioica*. Nature 431:67–71
- 1365 Sheth N, Roca X, Hastings ML, Roeder T, Krainer AR, Sachidanandam R (2006) Comprehensive
 1366 splice-site analysis using comparative genomics. Nucleic Acids Res 34:3955–3967
- 1367 Somorjai IML, Martí-Solans J, Diaz-Gracia M, Nishida H, Imai KS, Escriva H, Cañestro C, Albalat
 1368 R (2018) Wnt evolution and function shuffling in liberal and conservative chordate genomes.
 1369 Genome Biol 19:98
- 1370 Soviknes AM, Glover JC (2007) Spatiotemporal patterns of neurogenesis in the appendicularian
 1371 *Oikopleura dioica*. Dev Biol 311:264–275
- 1372 Soviknes AM, Glover JC (2008) Continued growth and cell proliferation into adulthood in the
 1373 notochord of the appendicularian *Oikopleura dioica*. Biol Bull 214:17–28
- 1374 Soviknes AM, Chourrout D, Glover JC (2005) Development of putative GABAergic neurons in the
 1375 appendicularian urochordate *Oikopleura dioica*. J Comp Neurol 490:12–28
- 1376 Soviknes AM, Chourrout D, Glover JC (2007) Development of the caudal nerve cord, motoneu-
 1377 rons, and muscle innervation in the appendicularian urochordate *Oikopleura dioica*. J Comp
 1378 Neurol 503:224–243
- 1379 Spada F, Steen H, Troedsson C, Kallesoe T, Spriet E, Mann M, Thompson EM (2001) Molecular
 1380 patterning of the oikoplasmic epithelium of the larvacean tunicate *Oikopleura dioica*. J Biol
 1381 Chem 276:20624–20632
- 1382 Stach TG (2009) Anatomy of the trunk mesoderm in tunicates: homology considerations and
 1383 phylogenetic interpretation. Zoomorphology 128:97–109
- 1384 Stach T, Anselmi C (2015) High-precision morphology: bifocal 4D-microscopy enables the
 1385 comparison of detailed cell lineages of two chordate species separated for more than 525 million
 1386 years. BMC Biol 13:113
- 1387 Stach T, Winter J, Bouquet JM, Chourrout D, Schnabel R (2008) Embryology of a planktonic
 1388 tunicate reveals traces of sessility. Proc Natl Acad Sci USA 105:7229–7234
- 1389 Stemple DL (2005) Structure and function of the notochord: an essential organ for chordate
 1390 development. Development 132:2503–2512
- 1391 Sulston JE, Schierenberg E, White JG, Thomson JN (1983) The embryonic cell lineage of the
 1392 nematode *Caenorhabditis elegans*. Dev Biol 100:64–119

- Thompson EM, Kallesøe T, Spada F (2001) Diverse genes expressed in distinct regions of the trunk epithelium define a monolayer cellular template for construction of the oikopleurid house. *Dev Biol* 238:260–273 1393–1395
- Tomita M, Shiga N, Ikeda T (2003) Seasonal occurrence and vertical distribution of appendicularians in Toyama Bay, southern Japan Sea. *J Plankton Res* 25:579–589 1397
- Torres-Aguila NP, Martí-Solans J, Ferrandez-Roldan A, Almazan A, Roncalli V, D’aniello S, Romano G, Palumbo A, Albalat R, Cañestro C (2018) Diatom bloom-derived biotoxins cause aberrant development and gene expression in the appendicularian chordate *Oikopleura dioica*. *Commun Biol* 1:121 1400–1401
- Troedsson C, Bouquet J-M, Aksnes DL, Thompson EM (2002) Resource allocation between somatic growth and reproductive output in the pelagic chordate *Oikopleura dioica* allows opportunistic response to nutritional variation. *Mar Ecol Prog Ser* 243:83–91 1403–1404
- Troedsson C, Bouquet J-M, Lobon C, Novac A, Nejstgaard J, Dupont S, Bosak S, Jakobsen H, Romanova N, Pankoke L, Isla A, Dutz JR, Sazhin A, Thompson E (2013) Effects of ocean acidification, temperature and nutrient regimes on the appendicularian *Oikopleura dioica*: a mesocosm study. *Mar Biol* 160:2175–2187 1405–1408
- Uren AG, O’rourke K, Aravind LA, Pisabarro MT, Seshagiri S, Koonin EV, Dixit VM (2000) Identification of paracaspases and metacaspases: two ancient families of caspase-like proteins, one of which plays a key role in MALT lymphoma. *Mol Cell* 6:961–967 1409–1411
- Uye S-I, Ichino S (1995) Seasonal variations in abundance, size composition, biomass and production rate of *Oikopleura dioica* (Fol) (Tunicata: Appendicularia) in a temperate eutrophic inlet. *J Exp Mar Biol Ecol* 189:1–11 1412–1414
- Volff JN, Lehrach H, Reinhardt R, Chourrout D (2004) Retroelement dynamics and a novel type of chordate retrovirus-like elements in the miniature genome of the tunicate *Oikopleura dioica*. *Mol Biol Evol* 21:2022–2033 1415–1417
- Walkusz W, Storemark K, Skau T, Gannefors C, Lundberg M (2003) Zooplankton community structure; a comparison of fjords, open water and ice stations in the Svalbard area. *Pol Polar Res* 24:149–165 1418–1419
- Wang K, Dantec C, Lemaire P, Onuma TA, Nishida H (2017) Genome-wide survey of miRNAs and their evolutionary history in the ascidian, *Halocynthia roretzi*. *BMC Genomics* 18:314 1421–1422
- Wegner M (2010) All purpose Sox: the many roles of Sox proteins in gene expression. *Int J Biochem Cell Biol* 42:381–390 1423–1424
- Weill M, Philips A, Chourrout D, Fort P (2005) The caspase family in urochordates: distinct evolutionary fates in ascidians and larvaceans. *Biol Cell* 97:857–866 1425–1426
- Welsch U, Storch V (1969) On the fine structure of the chorda dorsalis in lower chordata. (*Dendrodoa grossularia* (v. Beneden) and *Oikopleura dioica* Fol). *Z Zellforsch Mikrosk Anat* 93:547–549 1427–1429
- Yadette F, Butcher S, Forde HE, Campsteijn C, Bouquet JM, Karlsen OA, Denoed F, Metpally R, Thompson EM, Manak JR, Goksoyr A, Chourrout D (2012) Conservation and divergence of chemical defense system in the tunicate *Oikopleura dioica* revealed by genome wide response to two xenobiotics. *BMC Genomics* 13:55 1430–1433
- Zarsky V, Tachezy J (2015) Evolutionary loss of peroxisomes-not limited to parasites. *Biol Direct* 10:74 1434–1435

Author Queries

Chapter No.: 4 462645_1_En

Query Refs.	Details Required	Author's response
AU1	Please check the sentence "We pay special attention to..." for clarity.	
AU2	Please check whether the edit made to the sentence "The choice of a particular model..." is appropriate.	
AU3	Please check the hierarchy of the section headings and confirm if correct.	
AU4	The citation "Aravena (2002)" has been changed to "Aravena and Palma (2002)" to match the author name/date in the reference list. Please check if the change is fine in this occurrence and modify the subsequent occurrences, if necessary.	
AU5	Please check whether the output of Tables 4.1 and 4.2 are appropriate.	
AU6	Please check whether the edit made to the sentence "Lineage-specific duplicates might ..." is appropriate.	
AU7	Please check edit made to the sentence "In this section, ..." is appropriate.	
AU8	Please check whether "faithful" should be "efficient" in the sentence "Because the aNHEJ system...".	
AU9	Please check whether the edit made to the sentence "Overall, it is through that the loss ..." is appropriate.	
AU10	Please provide updated information for the references "Coppola et al. (2019), Mikhaleva et al. (2015)", if applicable.	